Isotopic approaches to quantify root water uptake: a review and comparison of methods

Youri Rothfuss[1], Mathieu Javaux[1,2]

[1]Institute of Bio- and Geosciences, IBG-3 Agrosphere, Forschungszentrum Jülich GmbH, Jülich, 52425, Germany
5 [2]Earth and Life Institute, Environnemental Sciences (ELIE), Université catholique de Louvain (UCL), Louvain-la-Neuve, 1348, Belgium

Correspondence to: Youri Rothfuss (y.rothfuss@fz-juelich.de)

Abstract. Plant root water uptake (RWU) has been documented for the past five decades from water stable isotopic analysis. By comparing the (hydrogen or oxygen) stable isotopic composition of plant xylem water to those of potential contributive
10 water sources (e.g., water from different soil layers, groundwater, water from recent precipitation or from a nearby stream) studies could determine the relative contributions of these water sources to RWU.

In this paper, the different methods used for locating / quantifying relative contributions of water sources to RWU (i.e., graphical inference, statistical (e.g., Bayesian) multi-source linear mixing models) are reviewed with emphasis on their respective advantages and drawbacks. The graphical and statistical methods are tested against a physically based analytical
15 RWU model during a series of virtual experiments differing in the depth of the groundwater table, the soil surface water status, and the plant transpiration rate value. The benchmarking of these methods illustrates the limitations of the graphical and statistical methods while it underlines the performance of one Bayesian mixing model. The simplest two end-member mixing model is also successfully tested when all possible sources in the soil can be identified to define the two end-members and compute their isotopic compositions. Finally, the authors call for a development of approaches coupling
20 physically based RWU models with controlled conditions experimental setups.

Keywords

Root water uptake; hydraulic redistribution; hydraulic lift; water stable isotopologues; isotope mixing model; physically based root water uptake model

25 **1 INTRODUCTION**

Understanding how the distribution of soil water and root hydraulic architecture impact root water uptake (RWU) location and magnitude is important for better managing plant irrigation, developing new plant genotypes more tolerant to drought or

tackling ecological questions in water-limited ecosystems, such as the competition for soil water by different plants (Javaux et al., 2013).

RWU - defined as the amount of water abstracted by a root system from soil over a certain period of time - is principally driven by transpiration flux taking place in the leaves. Its magnitude depends on the atmospheric evaporative demand and stomatal opening. The latter depends amongst others on leaf water status and stress hormonal signals from the roots transported to the leaves (e.g., Huber et al., 2015; Tardieu and Davies, 1993). Leaf water status and stress hormonal signals are related to the soil water potential distribution and to the plant hydraulic architecture (Huber et al., 2015). The distribution of RWU is very variable in time and space, depends on the presence of roots and their ability to extract water. This ability is a function of radial conductivity but axial conductance may also limit water flow in younger roots or when cavitation occurs. The flux of water depends also on soil water availability, i.e., the ability of the soil to provide water at the plant imposed rate (Couvreur et al., 2014): a highly conductive root segment will not be able to extract water from a dry soil. Locally, this is the difference of water potential between the root and the soil which drives RWU, and its magnitude is controlled by the radial hydraulic resistances in the rhizosphere, at the soil root interface and in the root system (Steudle and Peterson, 1998). The actual RWU profile is thus a combination of different aspects: the root's ability to extract water (characterized by the amount of roots and their hydraulic properties), the ability of the soil to fulfill the plant water demand, and the water potential difference between soil and root (Couvreur et al., 2014).

Plants have numerous mechanisms to cope with heterogeneous soil water distribution, e.g., adaptive root growth, adaptive root conductivity or exudation (Carminati et al., 2016). A particular process, which has attracted the attention of plant breeders and ecologists is the ability of plants to extract water from non or less water limited soil areas with potentially low root lengths densities (RLD [L L^{-3}], usually expressed in cm root per cm^3 soil), known as root water uptake compensation (Heinen, 2014). To describe the RWU rate in soils, we will use the root water uptake flow per volume of soil, defined as S [L^3 T^{-1} L^{-3}] described as a sink term in the Richards equation. According to Couvreur et al. (2012), root compensation is defined as the process that decreases or increases RWU at a certain location compared to the water uptake from that location when the soil water potential would be uniform in the root zone. Thus, the distribution of the $S(x,y,z)$ is a sum of two spatially distributed components:

$$S(x, y, z) = S_{\mathrm{uniH}}(x, y, z) + S_{\mathrm{comp}}(x, y, z) \tag{1}$$

where x, y and z are the 3D spatial coordinates, S_{uniH} is a term proportional to the root distribution and S_{comp} the compensatory part of the RWU distribution. The first term on the right-hand side of Eq. (1) is always positive while the second one can be either positive or negative. Figure 1 illustrates how this equation affects S distribution in a one-dimensional (1D) space. When there is no compensation ($S_{\mathrm{comp}}(x,y,z) = 0$), the RWU distribution follows the root distribution (i.e., highest at the surface and lowest in the deepest layer, Fig. 1a). When $S_{\mathrm{comp}}(x,y,z) < 0$ but its absolute value is lower than $S_{\mathrm{uniH}}(x,y,z)$, then $S(x,y,z)$ is positive and different from the root vertical distribution. In case $S_{\mathrm{uniH}}(x,y,z)$ is small, as in Fig. 1c, $S_{\mathrm{comp}}(x,y,z)$ can locally be higher in absolute value and $S(x,y,z)$ can be locally negative which implies that there is a water

efflux out of the root (called "Hydraulic redistribution" or "Hydraulic lift" in this particular case, Caldwell and Richards, 1989; Dawson, 1993; Kurz-Besson et al., 2006).

Despite its importance, datasets with measurements of RWU are lacking. This is related to the difficulty of measuring root and soil water fluxes. Often soil water content change is used as a proxy for RWU. Yet, as change of soil water content with time is not due to root extraction only (i.e., soil water redistribution can also occur), the assessment of RWU based on water content distribution alone is not possible in conductive soils (Musters and Bouten, 2000). Rather, the full soil water flow equation accounting for root uptake and soil water redistribution must be solved in an inverse mode, and, with an accurate knowledge of soil and root properties RWU distribution can be inferred (Guderle and Hildebrandt, 2015; Hupet et al., 2002; Musters and Bouten, 1999; Vandoorne et al., 2012). Nuclear magnetic resonance (NMR) imaging has been suggested as an adequate technique to measure water flow velocity in xylem vessels but no application exists yet on living roots in soils (Scheenen et al., 2000). More recently, Zarebanadkouki et al. (2012) could measure for the first time RWU in porous media by combining a tracer experiment (i.e., deuterated water) monitored by neutron tomography with inverse modelling of a transport equation. Yet, this was performed under controlled conditions while there is no standard method to monitor three dimensional water uptake distribution of growing roots *in situ*. In woody plants, in which roots are thick enough, Nadezhdina et al. (2010; 2012; 2015) used sap flow measurements in roots to quantify hydraulic redistribution.

Since the seminal work of Zimmermann et al. (1967) which reported that RWU of *Tradescantia fluminensis* occurred in the absence of fractionation against water oxygen stable isotope, water stable isotopologues ($^1H^2H^{16}O$ and $^1H_2{}^{18}O$) have been frequently used to identify and quantify RWU in soils through the measurements of their natural (and artificial) isotopic abundances. Methods include simple graphical inference to more sophisticated statistical methods, i.e., two-end members and multi-source linear mixing models. While the former attempts to locate the "mean root water uptake" in the soil, the latter category of methods provides profiles of relative contributions to transpiration flux across a number of defined soil layers.

This present paper has three objectives: (i) performing a literature review on the use of water stable isotopes to assess RWU; (ii) presenting the methods for translating the isotopic information into RWU profiles (i.e., graphical inference and statistical multi-source linear mixing models); and (iii) comparing these methods with a series of virtual experiments differing in the water and isotopic statuses in the soil and the plant. Prior to the review and inter-comparison, the paper reports on the mechanisms at the origin of the spatiotemporal dynamics of natural isotopic abundances in soil and on the background knowledge of isotopic transfer of soil water to and from roots. Finally, we evoke opportunities offered by novel isotopic monitoring tools which provide unpreceded high frequency isotopic measurements, and call for a development of approaches making use of physically based models for RWU determination.

2 FLOW OF ISOTOPOLOGUES IN THE SOIL-PLANT SYSTEM

In a study that laid the basis for future work in isotopic ecohydrology, Zimmermann et al. (1967) provided a steady-state analytical solution for soil water isotopic composition (δ_S, expressed in ‰ relative to the Vienna Standard Median Ocean Water international (VSMOW) isotope reference scale, Gonfiantini, 1978) in a water-saturated isothermal bare sand profile
5   from which water evaporated at a constant rate. Under these steady-state and isothermal conditions, the upward (convective) liquid flux of isotopologues, triggered by evaporation (E) and rising from deeper layers equals the downward (diffusive) isotopic flux from the evaporating surface which is enriched in the heavy stable isotopologues due to evaporation. Furthermore, by conservation of mass, the isotopic composition of evaporation equals that of its source (e.g., groundwater), i.e., $\delta_E = \delta_{source}$. A profile is obtained (Fig. 2a, dark blue line) whose exponential shape depends on boundary conditions, i.e.,
10   the source water and surface water isotopic compositions (δ_{source} and δ_{surf}), the diffusion coefficient of the isotopologues in water, and of a soil "tortuosity factor", conceptually defined as the ratio of the geometrical to actual water transport distance. Barnes and Allison (1983) extended this formulation to a non-saturated sand column evaporating at isotopic steady state. In this case, the evaporating surface (i.e., the liquid-vapor interface) can be located below the soil surface and splits the profile into two regions where isotopic transport predominantly occurs either in the vapor phase above or in the liquid phase below
15   it. In the "vapor region", relative humidity generally is still close to unity for sand total water potential below 15 bars. At isotopic steady state, the maximal isotopic enrichment is at the evaporation front (δ_{EF} at soil depth z_{EF}) and can be simulated with the Craig and Gordon (1965) model. The isotopic composition of the soil residual adsorbed water in the "vapor region" above the evaporation front can be obtained by assuming thermodynamic equilibrium conditions and by applying Fick's law, and is shown to decrease linearly towards the value of the liquid water at the soil surface which is at thermodynamic
20   equilibrium with the ambient atmospheric water vapor (Fig. 2a, light blue line). Finally, note that Rothfuss et al. (2015) argued that, at transient state ($\delta_E \neq \delta_{source}$), the maximal isotopic enrichment in the soil profile might not point to the location of the evaporation front. Instead, they proposed that the depth where the steepest gradient in the isotopic profile is observed corresponds to the evaporation front.

In a two-dimensional (δ^{18}O, δ^2H) space, liquid soil water sampled below the evaporation front will plot on an "evaporation
25   line" with a slope typically lower than six and greater than two, depending on atmospheric and isotopic forcing, as a result of kinetic processes during evaporation. Above the evaporation front and at isotopic steady-state, soil liquid water is in equilibrium with a mixture of atmospheric water vapor (δ^{18}O-δ^2H slope ~8) and evaporated soil water vapor rising from the evaporation front ($2 < \delta^{18}$O-δ^2H slope < 6) (Sprenger et al., 2016). As a result, an intermediate value for the slope is expected, depending on the mixing ratio of atmospheric water vapor to evaporated soil vapor at a given soil depth. Finally,
30   under natural conditions, the δ_S profile is not solely a result of isotopic fractionation but is as well highly impacted both spatially and temporally by input precipitation isotopic composition through modification of the upper boundary condition (δ_{surf}).

As opposed to the removal of water vapor by evaporation, RWU has been described in a number of studies and over a wide variety of plant species not to be associated with (kinetic) isotopic fractionation (Bariac et al., 1994; Dawson and Ehleringer, 1993; Thorburn et al., 1993; Walker and Richardson, 1991; Washburn and Smith, 1934; White et al., 1985; Zimmermann et al., 1967). Consequently, for plants growing in homogeneous external conditions, e.g., in hydroponic solution, root xylem sap water and external water have the same isotopic compositions. In natural soils where the liquid phase is not homogeneous and a vertical gradient of isotopic composition due to evaporation exists, the root system takes up water at different depths having thus different isotopic compositions.

Assuming that water transport time in roots is negligible, the isotopic concentration of the xylem sap water at the root tiller (C_{Ti} [M L^{-3}]) can be modeled as the weighted average of the product of the soil water isotopic concentration (C_S [M L^{-3}]) and $S(x,y,z)$:

$$C_{Ti} = \frac{\int_{x,y,z} C_S(x,y,z) \cdot S(x,y,z) \cdot dx \cdot dy \cdot dz}{\int_{x,y,z} S(x,y,z) \cdot dx \cdot dy \cdot dz} = \frac{\int_{x,y,z} C_S(x,y,z) \cdot S(x,y,z) \cdot dx \cdot dy \cdot dz}{J_{Ti}} \tag{2}$$

with J_{Ti} [L^3 T^{-1}] the xylem sap flux at the root tiller. Following Braud et al. (2005):

$$C = \rho \cdot R_{ref} \frac{M_i}{M_w}(\delta + 1) \tag{3}$$

with ρ [M L^{-3}] the volumetric mass of water, R_{ref} [-] the Vienna-Standard Mean Ocean Water (V-SMOW) hydrogen or oxygen isotopic ratio, M_w and M_i [M L^{-3}] the molar masses of $^1H_2^{16}O$ and isotopologue ($^1H^2H^{16}O$ or $^1H_2^{18}O$), respectively, the xylem sap water isotopic composition at the root tiller δ_{Ti} [-, expressed in ‰] can be expressed as:

$$\delta_{Ti} = \frac{\int_{x,y,z} \delta_S(x,y,z) \cdot S(x,y,z).dx \cdot dy \cdot dz}{J_{Ti}} \tag{4a}$$

with $\delta_S(x,y,z)$ [-, expressed in ‰] the isotopic compositions of soil water at coordinates (x,y,z). Mostly, a one dimensional description of RWU is used assuming that δ_S and RWU do not vary in the horizontal direction and δ_S is obtained for discrete soil layers of depths z_j ($j \in [1,n]$) and thickness $\Delta z_j = z_{j+1} - z_j$. It is usually further hypothesized that J_{Ti} equals the transpiration flux T [L^3 T^{-1}] (low to no plant capacitance or phloem-xylem contact):

$$\delta_{Ti} = \frac{\sum_{j=1,n} \delta_S(z_j) \cdot S(z_j) \cdot \Delta z_j}{\sum_{j=1,n} S(z_j) \cdot \Delta z_j} = \frac{\sum_{j=1,n} \delta_S(z_j) \cdot S(z_j) \cdot \Delta z_j}{q_{Ti}} \tag{4b}$$

where $q_{Ti} = J_{Ti}/(\Delta x \Delta y) = T/(\Delta x \Delta y)$ represents the sap flow rate in the root tiller per unit surface area [L T^{-1}].

δ_{Ti} can be accessed at different locations in the plant depending on the species, but the sampling location should not be affected by evaporative enrichment in heavier isotopologues or back-diffusion of the isotopic excess accumulated at the sites

of transpiration (stomatal chambers) in the leaf. For grasses and nonwoody plants, this is done by sampling the root crown (e.g., Leroux et al., 1995), the aerial nodal roots (e.g., Asbjornsen et al., 2007), the meristematic petiole, or else the collars (e.g., tillers) at the base of the plant (e.g., Dawson and Pate, 1996; Sánchez-Perez et al., 2008). In the case of ligneous plants the fully suberized stem (Asbjornsen et al., 2007) or sapwood (e.g., White et al., 1985) is sampled. On the other hand, δ_S is

5 usually measured by sampling soil profiles destructively. Finally, water from plant and soil is predominantly extracted by cryogenic vacuum distillation (Araguás-Araguás et al., 1995; Ingraham and Shadel, 1992; Koeniger et al., 2011; Orlowski et al., 2013; West et al., 2006).

Lin and Sternberg (1992) and Ellsworth and Williams (2007), amongst other authors, reported however that for some xerophyte (plants adapted to arid environments, e.g., *Prosopis velutina* Woot.) and halophytes species (plants adapted to

10 saline environments, e.g., *Conocarpus erecta* L.), and mangrove species (e.g., *Laguncularia racemosa* Gaert.), RWU led to fractionation of water hydrogen isotopologues. For mangrove species, it was hypothesized that the highly developed Casparian strip of the root endodermis would force water moving symplastically (i.e., inside the cells) and therefore crossing cell membranes (Ellsworth and Williams, 2007). Water aggregates are then dissociated into single molecules to move across these membranes. This demands more energy for $^1H^2H^{16}O$ than for $^1H_2^{16}O$ and $^1H_2^{18}O$, thus preferentially affects $^1H^2H^{16}O$

15 tranport and leads to a situation where xylem sap water is depleted in this isotopologue with respect to source water. Meanwhile, this affects to a much lesser extent $^1H_2^{18}O$ transport, so that no detectable isotopic fractionation of water oxygen isotopologues is observed. It can be concluded that, for the majority of the studied plant species, either RWU does not lead to isotopic fractionation or its magnitude is too low to be observable.

Finally, plant water samples will, similarly to soil water samples, fall onto an "evaporation line" of a slope lower than eight

20 in a two-dimensional ($\delta^{18}O$, δ^2H) space (Javaux et al., 2016).

3 LITERATURE REVIEW

By entering the search terms ((("root water uptake" or ("water source" and root) or "water uptake") and isotop*) into the ISI Web of Science search engine (webofknowledge.com), 159 studies published in the last 32 years were identified (see a listing of all studies in the supplementary materials). Cumulative number of articles as a function of publication year follows

25 an exponential shape: in average over the period 1985-2014, number of publications per year increased for about 0.3 and reached 8 (2014). In both years 2015 and 2016, the isotopic method for locating or partitioning water sources to RWU gained significantly more attention with 20 publications per year (Fig. 3a).

When sorting plant species simply by their form and height, it appears that trees are the most studied group of plants (present in about 60% of the studies), followed by annual and perennial grasses (21%) and shrubs (e.g., desert and mangrove species,

30 21%) (Fig. 3b). Only 15% of the publications study RWU in agricultural systems (e.g., maize, wheat, millet, rice), which is reflected by the small portion of peer-reviewed journals of which the category is listed under "Agronomy and Crop Science"

(8%) by Scimago Journal & Country Rank (www.scimagojr.com). This is a rather surprising finding given the fact that drought stress is considered as a major threat for crop yields and that RWU is a crucial mechanism to sustain drought periods. "Soil Science" is a relatively underrepresented category with 8% as well. This is corroborated by the fact that 27% of the studies do not report any information about soils (e.g., texture, FAO class, structure, particle size distribution, or

5 physical properties) (Fig. 3c). In comparison, the "Ecology" and "Ecology, Evolution, Behavior and Systematics" categories are significantly more represented with 22% of the studies altogether.

Four classes of methods for RWU analysis on basis of isotopic information emerged from our analysis (Fig. 3d). In a first one, representing 46% of the studies, RWU is either located in a specific soil layer using the method of "direct inference" (Brunel et al., 1995) or in some water pool (or water "source", not to be mistaken with the concept of water source defined in

10 the previous section), e.g., groundwater, soil water, or rainwater (Andrade et al., 2005; Beyer et al., 2016; Roupsard et al., 1999). In a second class (32% of the studies), relative contributions of at least three water sources to RWU are determined using multi-source mixing models (e.g., MixSir and MixSIAR, Moore and Semmens, 2008, representing 2% of the studies; SIAR, Parnell et al., 2013, 5%; IsoSource, Phillips and Gregg, 2003, 21%). In a third class (18% of the studies), relative contributions of two particular water sources (e.g., water in two distinct soil layers, or groundwater versus recent

15 precipitation etc.) to RWU are calculated "by hand" with a two end-member linear mixing model (Araki and Iijima, 2005; Dawson and Pate, 1996; Schwendenmann et al., 2015). Note that classes two and three (representing 50% of the studies) are both based on end-member mixing analysis (EMMA) (Barthold et al., 2011; Christophersen and Hooper, 1992) and will be further pooled into "statistical approach" in section 3.2 of this study.

In a fourth class, only accounting for 4% of the studies, assessments are provided using physically based analytical

20 (Boujamlaoui et al., 2005; Ogle et al., 2014; Ogle et al., 2004) or numerical (i.e., SiSPAT-Isotope, Rothfuss et al., 2012; HYDRUS-1D, Stumpp et al., 2012; Sutanto et al., 2012) models, therefore leading to an estimation of a RWU profile variable in time.

Note that all methods have in common to use an inverse modelling approach: the RWU distribution is obtained by optimizing model input parameters until the simulated δ_{Ti} and/or the simulated δ_S profiles fit to the isotopic measurements.

25 One important feature of the three first classes of methods is that they consider soil water isotopic transport flow to be negligible for the duration of the experiment. Numerical models such as HYDRUS-1D and SiSPAT-Isotope on the other hand take this into account in the computation of RWU profiles. The three first methods also differ from the last one by the fact that they only give fractions of RWU instead of absolute RWU rates changing in time and space.

61% of the studies based their estimation of location or quantification of relative contributions on measurement of either δ^2H

30 or $\delta^{18}O$, i.e., in a single isotope framework, while 25% used both δ^2H and $\delta^{18}O$ (i.e., in a dual isotope framework). In the remaining studies, both isotopic compositions were measured and used to provide two separate estimates of relative contribution distributions even though δ^2H or $\delta^{18}O$ distributions were strongly linked (see section 2). This last approach is in the present study referred as "double single" (see supplementary materials). The vast majority of the studies (82%) took

advantage of natural isotopic abundances while the rest (18%) applied labelling pulses to the soil (either in the profile or at the soil boundaries, e.g., the soil surface and groundwater) to infer RWU from uptake of labeled water.

To summarize, we observe that isotopic analyses have mainly been used up to now to assess water sources under natural ecosystems mainly using statistical approaches. On the opposite, these techniques have not been used much to investigate RWU of crops. It is also observed that the use of water isotope composition datasets combined with explicit physical models is lacking. In the next sections, we analyze the main methods currently use to retrieve RWU with isotopic water composition and compare the different methods. Table 1 summarizes 21 particular isotopic studies that use either one of the first three classes of methods (i.e., accounting for about 96% of the published studies), while class four (physically based RWU models) will be treated separately in section 4 of this study. These 21 studies were chosen according to either the number of citations and contribution importance (for studies published before 2015) or to the novelty of the publications (publication year $\geq$ 2015).

3.1 Graphical inference (GI)

This straightforward approach first proposed by Brunel et al. (1995) and applied by, e.g., Leroux et al. (1995), Weltzin and McPherson (1997) (Table 1) and else by Midwood et al. (1998), Armas et al. (2012), and Isaac et al. (2014) (see supplementary materials) defines the "mean root water uptake depth" $\bar{z}$, as the depth where $\delta_S = \delta_{Ti}$. $\bar{z}$ conceptually indicates to the soil depth where the plant root system, represented as one unique root, would extract water from.

There are cases where $\bar{z}$ cannot be unambiguously identified (e.g., $\bar{z}_1$ and $\bar{z}_2$ of case 2, Fig. 2b) due to the non-monotonic character of the δ_S profile (shown in black dashed line, case 2 of Fig. 2b). In order to define a mean RWU depth for such a case one can derive a monotonously decreasing δ_S profile by smoothing the profile (shown as symbols in Fig. 2b), e.g., by averaging δ_S in a number of layers using the following mass balance:

$$\delta_{S,J} = \frac{\sum_{j \leq J} \delta_S(z_j) \cdot \theta(z_j) \cdot \Delta z_j}{\sum_{j \leq J} \theta(z_j) \cdot \Delta z_j} \tag{5}$$

where J represents the set of depths that belong to the Jth soil layer, with θ [L^3 L^{-3}] and Δz_j [L] the soil volumetric water content and thickness of the soil layer centered around depth z_j. Due to this smoothing, the vertical resolution may be drastically reduced. In the example presented in Fig. 2b where a uniform θ profile is assumed, the $\delta_{S,J}$ profile intersects with the vertical line of value δ_{Ti} deeper than for the initially non-monotonic δ_S profile, i.e., $\bar{z}$ (case 2, integrated δ_S profile) < $\bar{z}_2 < \bar{z}_1$. Some authors rule out solutions in case of multiple mean RWU depths, e.g., by excluding the $\bar{z}$ solutions where soil water content was low and/or soil water potential was high in absolute value (e.g., Li et al., 2007; see Table 1).

Note that while Eq. (5) provides a representative value for the isotopic composition that would be measured in soil layer J as a function of those of the water in the set of depths, $\delta_{S,J}$ is however equivalent to the isotopic composition "sensed by the plant" only if the root profile is homogeneous, i.e., when RLD is constant over depth in that particular soil layer J.

The graphical inference method may not only provide $\bar{z}$ but also its uncertainty caused by the uncertainty in measuring δ_{Ti} (e.g., based on the precision of the isotopic analysis and/or sampling natural variability, shown as gray stripe in Fig. 2b). The steeper the soil water isotopic profile, the larger the uncertainty in determining $\bar{z}$ is. Figure 2b illustrates this with estimated minimum and maximum $\bar{z}$ for the monotonic δ_S profile and for the vertically averaged profile. In the latter case, the possible range of $\bar{z}$ is the largest. These ranges give first quantitative indication of variance around $\bar{z}$. Finally, for a complete "graphical assessment" of the variance of $\bar{z}$, one should consider the uncertainty associated with measurements of the δ_S profile (not shown here; for a complete assessment of errors associated with determination of δ_S, see Sprenger et al., 2015) as well.

3.2 Statistical approaches

3.2.1 Two end-member (TM) mixing model

The TM method is a particular case of end-member mixing analysis (EMMA) and is based on the concept that (i) a plant extracts water from two predominant water sources A and B (e.g., water in distinct upper and lower soil layers, or groundwater and recent precipitation water etc.) in given proportions, (ii) there is no isotopic fractionation during water uptake, and (iii) there is a complete mixing inside the plant of the contributing water sources A and B to RWU. The mass conservation for isotopologues gives:

$$J_{Ti}^i = J_A^i + J_B^i \tag{6a}$$

$$C_{Ti} \cdot J_{Ti} = C_A \cdot J_A + C_B \cdot J_B \tag{6b}$$

with J_A, J_B, and J_{Ti}, [L^3 T^{-1}] (respectively J_A^i, J_B^i, and J_{Ti}^i [M T^{-1}]) the fluxes of water (respectively isotopologues) originating from water sources A and B, and at the plant tiller. C_A, C_B, and C_{Ti} [M L^{-3}] are the water sources A and B, and xylem sap water measured isotopic concentrations. By introducing $x = J_A / J_{Ti}$ and following Eq. (3), Eq. (6b) becomes:

$$\delta_{Ti} = x \cdot \delta_A + (1-x) \cdot \delta_B \tag{7}$$

In this approach, δ_{Ti} is therefore defined as the mean value of the isotopic compositions of water sources A and B (δ_A and δ_B) weighted by the proportions to J_{Ti} of water volume extracted by the plant from water sources A and B, i.e., x and $(1 - x)$, respectively. The error associated with the estimation of x (σ_x [-, expressed in ‰]) can be calculated following Phillips and Gregg (2001):

$$\sigma_x^2 = \left(\frac{\partial x}{\partial(\delta_A)}\right)^2 \cdot \sigma_{\delta_A}^2 + \left(\frac{\partial x}{\partial(\delta_B)}\right)^2 \cdot \sigma_{\delta_B}^2 + \left(\frac{\partial x}{\partial(\delta_{xyl})}\right)^2 \cdot \sigma_{\delta_{Ti}}^2 \tag{8a}$$

$$\sigma_x = \sqrt{\sigma_x^2} = \frac{1}{(\delta_A - \delta_B)} \sqrt{\left(\sigma_{\delta_{Ti}}^2 + x^2 \cdot \sigma_{\delta_A}^2 + (1-x)^2 \cdot \sigma_{\delta_B}^2\right)} \tag{8b}$$

with σ_{δ_A}, σ_{δ_B}, and $\sigma_{\delta_{Ti}}$ the standard errors associated with the measurements of δ_A, δ_B, and δ_{Ti}, respectively. The sensitivity of Eq. (8b) to different values of σ_{δ_A}, σ_{δ_B}, and $\sigma_{\delta_{Ti}}$ can be tested by considering either minimal possible errors, i.e., the analytical precision of the isotopic analyser (e.g., isotope ratio mass spectrometer, laser-based spectrometer), or by taking additional errors involved with sampling procedure and vacuum distillation technique (see e.g., Rothfuss et al., 2010)

5   into account. Equation (8b) also shows that, independently of the values considered for σ_{δ_A}, σ_{δ_B}, or $\sigma_{\delta_{Ti}}$, σ_x is inversely proportional to $1/(\delta_A - \delta_B)$, indicating that the two end-members should have greatest possible isotopic dissimilarities for a low standard error of x. Therefore, it is especially important, e.g., for partitioning between water from an upper and lower portion of the soil profile, to properly define the thickness of these layers, so that they have distinct isotopic compositions, and that the difference is considerably larger than the precision of the isotopic measurements. Figure 4 shows for example

10   that when (i) x is evaluated at 10 % and (ii) σ_{δ_A}, σ_{δ_B}, and $\sigma_{\delta_{Ti}}$ are estimated being equal to 0.02 ‰ (dark blue solid line), $(\delta_A - \delta_B)$ should be greater than 0.75 ‰ (in absolute term) in order to reach a σ_x value lower than 5 %, i.e., more than 37 times the error made on δ_A, δ_B, and δ_{Ti}. To obtain the same standard error for x in case of a higher standard error on the estimation of δ_A, δ_B, and δ_{Ti} (e.g., σ_{δ_A}, σ_{δ_B}, and $\sigma_{\delta_{Ti}} = 0.1‰$), $(\delta_A - \delta_B)$ should be greater than 3.00 ‰ (in absolute term). This difference becomes much greater for σ_{δ_A}, σ_{δ_B}, and $\sigma_{\delta_{Ti}} = 1.00‰$ and reaches 42 ‰ (not shown in Fig. 4). This certainly

15   highlights the advantage of artificially labelling soil water with water enriched (or depleted) in heavy isotopologues for a more precise assessment of the relative contribution of soil water sources to RWU, as mentioned by Moreira et al. (2000). In another study, Bachmann et al. (2015) labelled the upper and lower portion of the soil profile in a natural temperate grassland with ^{18}O-enriched and ^{2}H-enriched water, respectively. They defined two distinct (upper and lower) soil water sources, for which they calculated the corresponding δ^2H or δ^{18}O on the basis of measured soil water isotopic profiles and

20   using Eq. (5). They could find evidence against the so-called hypothesis of "niche complementarity" regarding plant water use, which states that RWU of competitive plant species is spatially and temporally distinct, and that this distinction is stronger at high species richness. Figure 4 also illustrates that for given $(\delta_A - \delta_B)$, σ_{δ_A}, σ_{δ_B}, and $\sigma_{\delta_{Ti}}$ values, the "optimal x value" for a low σ_x is 50% (showed by the orange lines).

Table 1 displays a sample of studies that used the two end-member mixing approach. Authors could distinguish between

25   uptake of irrigation and precipitation water (Goebel et al., 2015), precipitation and groundwater (White et al., 1985), soil water and groundwater (McCole and Stern, 2007), or else between stream water and soil water (Dawson and Ehleringer, 1991; McDonnell, 2014). Thorburn and Ehleringer (1995) could for instance locate the dominant source for RWU, i.e., groundwater for their mountain and floodplain test-site and water from the soil between 0.3 and 0.4 meter depths for their cold desert test-site. Other Authors (e.g., Brunel et al., 1995) combined two mixing equations, i.e., one for each

30   isotopologue, into a single one or else, calculated the ratio of geometrical distances between δ_{Ti} and δ_A and between δ_{Ti} and δ_B in dual isotope (δ^{18}O and δ^2H) space (Bijoor et al., 2012; Feikema et al., 2010; Gaines et al., 2016). As infrared laser-

based spectrometry now enables simultaneous measurements of $\delta^{18}O$ and δ^2H at lower cost, we believe that this dual-isotope approach (referred as "D" in Table 1) will or should gain in importance in isotopic studies. This is especially useful when (i) under natural conditions the $\delta^{18}O$-δ^2H slope is not constant over depth (Sprenger et al., 2016) or (ii) in the context of pulse labelling experiments, which can artificially change the value of the $\delta^{18}O$-δ^2H slope at given locations in the soil profile. In

5   these cases, two independent mixing equations are obtained, one for each isotopologue.

3.2.2 Multi-source (MS) mixing models

When there are more than two identified plant water sources contributing to RWU, e.g., water from different layers j ($j \in [1, N]$) in soil the profile, Eq. (7) becomes:

$$\delta_{Ti} = \sum_{j=1}^{N} x_j \cdot \delta_{S,j} \tag{9}$$

10   with N the number of plant water sources (e.g., soil layers) and $\sum_{j=1}^{N} x_j = 1$. As there are more water sources than (number of

mixing equations + 1), there is not a unique solution but an infinite range of possible solutions. However, based on background information or knowledge, some of these solutions are not likely or possible. A range of solutions that is most likely based on prior information can be obtained using Bayesian methods. In the method proposed by Phillips and Gregg (2003), the isotopic composition calculated for each considered x_j combination (δ_{Ti}) is compared with the measured value

15   ($\delta_{Ti,m}$). The number of combinations depends on the value of the contributing increment (i, %, typically 5 or 10 %) and the combinations for which δ_{Ti} meets the following requirement are selected:

$$\delta_{Ti} \leq \left| \delta_{Ti,m} \pm \tau \right| \tag{10}$$

where τ [-, expressed in ‰], standing for "tolerance", usually accounts for precision of the isotopic measurements or possible errors during sampling and vacuum distillation steps. This multi-source mixing model approach strongly depends on τ and i,

20   which therefore should be carefully chosen by the user, e.g., a smaller i refines the analysis. For this, the program "IsoSource" (https://www.epa.gov/sites/production/files/2015-11/isosourcev1_3_1.zip) is available (Phillips et al., 2005). Wang et al. (2010) compared the outcome of the GI and MS approaches and came to the conclusion that even though the latter did not solve the non-uniqueness problem and provided diffuse patterns of frequency that were difficult to interpret in some cases (e.g., in case of a non-monotonic isotopic profile), it had the advantage over the former method of providing a

25   systematic and quantitative assessment of ranges of relative contributions. Romero-Saltos et al. (2005) extended the model of Phillips and Gregg (2003) by constraining RWU to follow a normal distribution within a delimited 50-cm soil vertical segment of one centimeter vertical resolution and centered around $\bar{z}$, the mean RWU depth. The location of this section and thus $\bar{z}$ is as well obtained by mass balance from inverse modelling similarly to IsoSource (see applications of Grossiord et al., 2014; Rossatto et al., 2013; Stahl et al., 2013).

Parnell et al. (2010) proposed to overcome two limitations of the approach of Phillips and Gregg (2003), i.e., its inability to (i) account for uncertainty in the estimations of δ_{Ti} and of the water sources isotopic compositions $\delta_{S,j}$, and to (ii) provide a optimal solution rather than ranges of feasible solutions. For doing this, they use a Bayesian framework (for details see Erhardt and Bedrick, 2013; Moore and Semmens, 2008; Parnell et al., 2013), which allows uncertainty in the x_j proportions and incorporates a residual error term ε_j (normally distributed with mean equal to zero and variance σ^2):

$$\delta_{Ti} = \sum_{j=1}^{N} x_j \cdot \delta_{S,j} + \varepsilon_j \qquad (9')$$

Note that the terms of (i) trophic enrichment factor (TEF [-, expressed in ‰], see, e.g., meta-analysis of Vanderklift and Ponsard, 2003) and (ii) isotope concentration dependency (Koch and Phillips, 2002; Phillips and Koch, 2002) originally incorporated in the formulation of Parnell et al. (2010) for other applications are not present in Eq. (9') since (i) no isotopic fractionation during RWU is assumed and (ii) isotope concentration dependency applies only for situations where isotopic compositions of different elements are measured and available.

Parnell et al. (2010) developed the program "Stable Isotope Analysis in R" (SIAR, https://cran.r-project.org/src/contrib/siar_4.2.tar.gz) in which the initial (*a priori*) x_j distribution is by default the Dirichlet distribution, of which information can be partly specified by the user. *A posteriori* x_j distribution is obtained by fitting the linear model to data via a Metropolis-Hasting (Hastings, 1970; Metropolis et al., 1953) Markov Chain Monte Carlo algorithm.

Prechsl et al. (2015) apply both graphical and Bayesian approaches to evaluate the shift in $\bar{z}$ and change of RWU profile following drought treatments (approx. 20 to 40 % precipitation reduction with transparent rainout shelters) in both extensively and intensively managed grasslands. From both approaches it appeared that a shift in $\bar{z}$ was inexistent or not observable from isotopic analyses. Another recent application of the Bayesian approach was performed by Volkmann et al. (2016b), who took advantage of a newly developed soil isotopic monitoring method to confront high frequency δ_S profiles time series to time series of δ_{Ti} (indirectly obtained from the isotopic measurement of the transpired water and assuming isotopic steady state, i.e., $\delta_{Ti} = \delta_T$) following a labelling pulse (see Table 1 for details on the study).

4 INTER-COMPARISON OF METHODS

We tested and compared the different methods (GI, TM, MS) during a series of virtual experiments in a single isotope framework ($\delta^{18}O$) and at natural isotopic abundance. Mean RWU depths (provided by the GI method) and x_j distribution (provided by the two end-member and multi-source mixing models) were determined from the δ_S profile and the δ_{Ti} value. For each virtual experiment the δ_S profile was prescribed to the different methods while δ_{Ti} was calculated with the physically based analytical RWU model (referred to as "Couv") of Couvreur et al. (2012).

It has been proved (Couvreur et al., 2012) that this model gives similar results than a 3D physically based model with detailed descriptions of the root architecture and of the water flow in soil and roots. In that sense, this is the best current

model existing nowadays to simulate water fluxes in a soil-plant system (based on biophysical considerations). Other current models make assumptions or use empirical relations to predict RWU, which are not based on bio-physical considerations only (Jarvis, 2011; Simunek and Hopmans, 2009). Obviously, we do not mean that the model of Couvreur et al. (2012) gives the reality but rather the best estimate of the water flow based on our physical knowledge.

5   The inter-comparison of models was performed using a single isotope (^{18}O) approach as the focus here was the differences of outcomes rather than the impact of the input isotopic data on these results. The reader is referred to Appendix B1 for a description of the model of Couvreur et al. (2012) and to Appendix B2 on how it was implemented for the inter-comparison.

4.1 Methodology

4.1.1 Scenario definition

10   We developed eight virtual plausible scenarios of soil-plant systems under different environmental conditions. For each scenario, we set one total soil water potential (H_S) profile and one soil water oxygen isotopic composition (δ_S) profile. These profiles resulted from the combination of a lower boundary condition, i.e., the depth of the groundwater table, and an upper boundary condition, i.e., the soil surface water status. The groundwater table (of water isotopic composition equal to -7‰) was either shallow at -1.25 m depth (prefix "Sh") or deep at -6 m depth (prefix "De"). The soil water potential was 15 considered to be at static equilibrium below the groundwater level. The soil surface was either dry under evaporative conditions (suffix "Dr"), or wet, e.g., shortly after a rain event (suffix "We"). For instance for the scenario "ShDr", we set the δ_S profile to be maximal at the surface, due to evaporation, and minimal from –0.5 m downward, due to the shallow groundwater table location. For the scenario "DeWe", on the other hand, the increase of δ_S towards the surface was not monotonic due to a recent precipitation event (of water isotopic composition equal to -7‰). Finally, we tested two different 20 values of plant transpiration rate (T) and leaf water potential (H_L) with each of these four combinations (i.e., ShDr, ShWe, DeDr, and DeWe). The transpiration rate was either low (e.g., relevant at night, $T = 0.01$ mm h^{-1}, suffix "_lT") or high ($T = 0.30$ mm h^{-1}, suffix "_hT"). All eight scenarios relied on a common measured root length density vertical distribution of *Festuca arundinacea*. Table 2 reports the input data. Note that, as hypothetized in Eq. (4b), transpiration and sap flow rates (i.e., per unit of surface area [L T^{-1}]) were considered as equal.

25   The objective was not to use an advanced numerical model such as, e.g., SiSPAT-Isotope or Soil-litter-iso, to produce these scenarios, but rather use synthetic information based on (i) experimental data and (ii) expert-knowledge which would ideally illustrate the performances or limitations of the different methods.

4.1.2 Setup of the models

The two end-member mixing approach (TM) was tested against the isotopic data for two different cases: (i) two conjoint soil 30 layers spreading from 0 – 0.225 m and 0.225 – 2.00 m and (ii) two disjoint soil layers spreading from 0 – 0.225 m and 1.75 – 2.00 m. The latter case was designed to evaluate the impact of lacunar soil isotopic information on the calculation of x, i.e.,

when not all potential water sources are properly identified. Representative values of water oxygen isotopic compositions for these soil layers ($\delta_{S,J}$, $J \in$ [I,II]) were obtained from the mass balance (Eq. (5)) after interpolation of the measured soil water content and δ_S profiles at a 0.01 m vertical resolution.

For the multi-source mixing models of Phillips and Gregg (2003) (IsoSource) and Parnell et al. (2010) (SIAR), the number of potential water sources was initially fixed to three, i.e., water from the soil layers I (0.000-0.050 m), II (0.050-0.225 m), and III (0.225-2.000 m). Upper and lower boundaries of these layers were defined to reflect the exponentially shaped (monotonic) δ_S profiles (experiments ShDr and DeDr) or to smooth the non-monotonic δ_S profiles observed during experiments ShWe and DeWe. IsoSource and SIAR were tested for eight soil layers (i.e., as many layers as measurement points, I: 0.000-0.020, II: 0.020-0.050, III: 0.050-0.110, IV: 0.110-0.225, V: 0.225-0.400; VI: 0.400-0.750, VII: 0.750-1.500, and VIII: 1.500-2.000 m) as well. Increment and tolerance in IsoSource were fixed to 10% and 0.25‰, respectively. Similarly to the TM approach, profiles of $\delta_{S,J}$ ($J \in$ [I,III] or [I,VIII]) were obtained from the mass balance (Eq. (5)) after interpolation of the measured soil water content and δ_S profiles at a 0.01 m vertical resolution.

Finally, for the SIAR model, uncertainty associated with δ_S measurements was set to 0.2 ‰ and the number of iterations was fixed to 500000 and number of iterations to be discarded to 50000.

For a detailed description of the inter-comparison methodology, the reader is referred to Appendix C.

4.2 Results and discussion

Figure 5 displays x_{Couv}, the $\dfrac{S(z)dz}{T/(\Delta x \cdot \Delta y)}$ ratios (solid colored lines) simulated by the analytical model of Couvreur et al. (2012) for the eight scenarios together with uncertainty (shaded areas) and the corresponding $\delta_{\text{Ti\_Couv}}$ (±1sd) (for a description on how uncertainty was assessed, refer to Appendix C). In general, at high T the compensation was negligible and the S profile was mainly proportional to the RLD profile (Fig. 5b, d, f, and h). The only exception was a soil with deep groundwater table and dry surface, where this dry layer limited RWU (DeDr_hT). At lower transpiration demand, the S profile predicted by the Couvreur et al. (2012) model generally differed from the RLD profile (Fig.5a, c , e, and g). This is due to the fact that the second term of Eq. (1) (i.e., S_{comp}, see Eq. (B4) and (B4') in Appendix B) was proportionally larger. Water uptake from the upper layer was always more than proportional to the RLD, when this layer was wetter, and vice versa. Water release to the soil (i.e., HR) was observed only for the soil with the deep groundwater table and dry upper layer (DeDr_hT, Fig. 5e). From the graphical method GI, either a single or two distinct solutions for $\bar{z}$ (displayed as gray-shaded horizontal stripes) were retrieved, depending on the monotonic/non-monotonic character of the δ_S profile, and ranged between −0.02 and −0.95 m.

Figure 6a displays the relative contribution to T of the uppermost layer $0 - 0.225$ m in case of two conjoint soil layers as computed with the TM approach and a comparison with the results of the analytical model. Except for the very last two virtual experiments with the deep groundwater table and wet upper layer at both low and high transpiration rates (i.e.,

DeWe_lT and DeWe_hT), there was a very good agreement between the analytical model and the two end-member mixing model: absolute difference between x_{Couv} and x_{TM} ranged between 1.5% (ShDr_lT) and 6.3% (ShDr_hT). For the experiment with the deep groundwater table and dry upper layer at low transpiration rate (DeDr_lT), the TM approach estimated that x was equal to 12.3% while the analytical model simulated hydraulic redistribution, i.e., excluded the layer $0 - 0.225$ m as potential source. The significant difference between results of the two models during experiments DeWe_lT and DeWe_hT and the higher standard error associated with x_{TM} (σ_x, displayed in the form of error bars in Figure 6) were due to the small difference between the isotopic compositions of the defined soil water sources $\delta_{S,I}$ (–6.0 ‰) and $\delta_{S,II}$ (–5.3 ‰) as illustrated in section §3.2.1. Figure 6b gives the relative contribution to T of the layer $1.75 - 2.00$ m in case of two disjoint soil layers, i.e., when not all potential water sources are accounted for into the calculation of $\delta_{S,I}$ and $\delta_{S,II}$. In this case there were important disparities between x_{TM} and x_{Couv}. The mean absolute difference between these two estimates was equal to 43,5 ($\pm$17.8)%. Omitting some of the potential water sources contributing to T had in this second case the consequence of artificially overestimating the contribution of the lowest layer. We therefore suggest to always attempting to fully characterize the soil isotopic profile before aggregating the isotopic information when defining the two water sources.

Figure 7 gives the relative contributions from soil layers I, II, and III (upper, middle, and lower panel, respectively) to T provided by IsoSource, the multi-source mixing model of Phillips and Gregg (2003) (x_{IsoS}, in %, displayed in the form of gray histograms) and by SIAR, the Bayesian method of Parnell et al. (2010) (x_{SIAR}, in %, gray probability density curves). The colored vertical lines are x_{I_Couv}, x_{II_Couv}, and x_{III_Couv}, the simulated $\dfrac{S(z)dz}{T/(\Delta x \cdot \Delta y)}$ ratios from layers I, II, and III. The color-shaded areas associated with x_{I_Couv}, x_{II_Couv}, and x_{III_Couv} refer to their uncertainty by accounting for the uncertainty of the input data. As for Fig. 5, δ_{Ti_Couv} is reported above each plot along with its standard deviation. x_{J_IsoS} probability distribution was observed to be either narrow (e.g., for the experiment with the deep groundwater table and dry upper layer at low transpiration rate – DeDr_lT / layer I, Fig. 7m) or broad (e.g., for the experiment with the deep groundwater table and wet upper layer at high transpiration rate – DeWe_hT / layer I), i.e., the range of the possible solutions for x_{J_IsoS} was relatively small or large (10 and 100% respectively for these two examples). In general, both IsoSource and SIAR results were in good agreement: the x_{SIAR} most frequent value (MFV, at the peak of the density distribution curve) was in most cases either located near the median value of the x_{IsoS} probability range (e.g., for the experiment with the shallow groundwater table and wet upper layer at low transpiration rate – ShWe_lT / layer I, Fig. 7g) or matched exactly the x_{IsoS} unique value (i.e., for the experiment with the deep groundwater table and dry upper layer at low transpiration rate – DeDr_lT / layer I, Fig. 7m). In contrast, the statistical methods succeeded best in providing x estimates similar to those of the model of Couvreur et al. (2012) in case of a shallow groundwater table and at low T only (Fig. 7a-c and g-i), thus when water availability was high and root compensation was low. In these cases, x_{I_Couv} was included in the estimated x_{I_IsoS} range and the mean absolute difference (MD) between x_{J_Couv} and x_{SIAR} MFV was equal to 8.6%. This difference was the greatest

(129.2%) for experiment DeDr_lT when hydraulic redistribution by the roots was simulated by the analytical model (Fig. 7m-o).

When considering eight soil layers instead of three, uncertainties in the assessment of the relative contributions to T as determined by IsoSource increased. The estimated probability ranges increased in most of the cases (results not shown). However, it considerably improved the results of the bayesian model: the mean absolute difference between x_{J_Couv} and the most frequent x_{SIAR} value was equal to 4.7% for the scenarios with a shallow groundwater table and low transpiration rate and equal to 52.1% in case of hydraulic redistribution by the roots (Table 3).

Independent of the number of defined soil layers, lowering the value of increment to 5% in IsoSource refined the analysis where the probability distribution was already narrow (i.e., in the case of a well identified x_{IsoS} value, e.g., Fig. 7m) while it produced distributions that were flatter and contained less gaps when no clear solutions had emerged before (results not shown). Artificially increasing the value of tolerance had the consequence that more solutions to Eq. (10) were found for each experiment / transpiration value / layer combinations and *vice versa* (results not shown). An increase or decrease of a factor 2 of the number of runs as well as the number of runs to be discarded from the analysis had only a marginal impact on the density distribution curves obtained with the SIAR model in the case of three or four soil layers.

The modelling exercise illustrated the disparities of outcome between the graphical method on the one hand and the statistical and mechanistic methods on the other: there simply cannot be a single or multiple "root water uptake depths" but rather a continuous RWU profile or statistical solutions of contribution to transpiration (provided by IsoSource and SIAR). Significant changes of δ_{Ti} do not necessarily mean important changes in the depth of RWU but rather slight (nevertheless significant) modification of the RWU profile. The authors believe that the relatively novel statistical tools presented in this review should therefore be preferred over the graphical inference method, especially since the two former are available as user-friendly programs and packages and do not require significant computing time, therefore can be run locally on a personal computer. As highlighted in this series of virtual experiments, the Bayesian method showed for the case of two and three soil layers much more convincing results than the method of Phillips and Gregg (2003). The Bayesian method was particularly efficient in the case of eight soil layers, illustrating the interest of reaching the best vertical resolution and maximizing the number of identified potential sources (Table 3). Note that no prior information on the relative contributions to T from the different soil layers was used when running the SIAR program, i.e., the authors opted for flat priors. This can be changed by the user, based on additional collected data such as, for instance, information of root architecture and function across the soil profile or information on soil hydraulic properties and water status.

One can show from this inter-comparison of methods that labelling of soil water in either [18]O or ^{2}H has potentials for improving the different methods presented here theoretically if water is taken up by the roots from the labeled region predominantly. However, this was never the case when considering the results of the analytical model. A dual isotope (^{18}O or ^{2}H) labelling pulse experiment that would artificially disconnect the strong link between $\delta^{18}O$ and δ^2H would on the other hand much more constrain the inverse problem and provide more accurate estimates.

5 CHALLENGES AND PROGRESSES

5.1 Off-line destructive versus on-line nondestructive isotopic measurements in plant and soil waters

For determination of δ_S, soil profiles are usually destructively sampled, typically with an auger down to a depth of a few centimeters (Rothfuss et al., 2010) to a few meters (Moreira et al., 2000) (see Table 1), depending on the depths of the root system and of the water table. The sampling depth resolution should, when possible, match the exponential decrease of isotopic composition (Wang et al., 2010) and it should capture sudden variations with time at the soil surface due to precipitation, i.e., be maximal at the surface and minimal deeper in the soil profile where isotopic dynamics are less pronounced. Not doing this can lead to a situation where source partitioning is not feasible from isotopic measurements. Under field conditions (i.e., ~95% of the studies reviewed in this work, summarized in Table 1) soil material is generally not a limiting factor, thus, can be sampled twice or thrice to average out or characterize lateral heterogeneity without significant disturbance of the soil.

Water from plant and soil materials is predominantly extracted by cryogenic vacuum distillation (Araguás-Araguás et al., 1995; Ingraham and Shadel, 1992; Koeniger et al., 2011; Orlowski et al., 2013; West et al., 2006). Accuracy of this extraction method was shown to be maximal at higher water content and for sandy soils and lower for soils with high clay content (e.g., Koeniger et al., 2011; West et al., 2006). In the latter case, extraction times should be longer and temperatures higher to mobilize water strongly bound to clay particles, which has a distinct isotopic composition from that of pore "bulk" water (Araguás-Araguás et al., 1995; Ingraham and Shadel, 1992; Oerter et al., 2014; Sofer and Gat, 1972).

Certainly one of the main limitations of all isotopic approaches for quantifying RWU is the destructive character of isotopic sampling (see section 3.1) and associated offline analyses (sections 2.2 and 2.3). This usually leads to poor spatial (maximum a few cm^2) as well as temporal (minimum hourly) resolution of the inferred results, when comparing with measuring frequency of other soil and plant state variables, e.g., soil water content and potential, and leaf water potential (section 3.2.2). In addition, one may question the representativeness of plant samples, in which tissues (and thus water) with very different water residence time is mixed.

Recently developed methods take advantage of laser-based spectroscopy which allows in-situ, on-line, and continuous isotopic measurements in the gas phase at high frequency. These methods rely on coupling a laser spectrometer (e.g., Wavelength-Scanned Cavity Ring-Down Spectroscopy – WS-CRDS, Picarro Inc., Santa Clara, CA, USA; Cavity-Ringdown Laser Absorption Spectroscopy – CRLAS and Off-Axis Integrated Cavity Output Spectroscopy - ICOS, Los Gatos Research, Los Gatos, USA) with specific soil gas sampling probes consisting of gas-permeable microporous polypropylene membranes or tubing. These membranes or tubing exhibit strong hydrophobic properties while their microporous structures allow the intrusion and collection of soil water vapor. Several authors (Gaj et al., 2015; Gangi et al., 2015; Herbstritt et al., 2012; Oerter et al., 2016; Rothfuss et al., 2013; Sprenger et al., 2015; Volkmann and Weiler, 2014) could determine the soil liquid water isotopic composition in a nondestructive (yet invasive) manner from that measured in the collected soil water vapor

considering thermodynamic equilibrium between vapor and liquid phase in the soil. In contrast to "traditional" isotopic methods, these novel isotopic monitoring methods have also the distinct advantage of determining soil liquid water isotopic composition at very low water content, since water vapor, in contrast to soil liquid water, is not limited for analysis. These novel methods allow a vertical resolution down to 1 cm and an approximately hourly time-resolution. However, they do not

5   allow horizontal resolution along the tube and the laser spectrometers could be, as pointed out by Gralher et al. (2016) for the specific case of a Picarro WS-CRDS, significantly sensitive to the carrier gas used. In their opinion papers, McDonnell (2014) and Orlowski et al. (2016a) urged for a comparison between methods, which was addressed by Orlowski et al. (2016b) and Pratt et al. (2016) (for vapor measurements only).

In the coming years, effort should be made towards developing novel methods for a direct and nondestructive determination

10   of δ_{Ti} based on the use of gas-permeable membranes, which was recently initiated for trees (Volkmann et al., 2016a). This should be further tested for other (non-woody) plant species. This will imply the major challenge of not disrupting the water columns in the active xylem vessels when installing such a membrane-based system. Another potential issue to be investigated is the species-specific extent of water exchange between xylem and phloem conductive tissues which might lead to isotopic "contamination" of the xylem sap water (Farquhar et al., 2007).

15   **5.2 Call for a coupled experiments-modelling approach for determination of plant water sources on the basis of isotopic data**

In order to fully benefit from the potential of water stable isotopic analysis as tools for partitioning transpiration flux, the authors call for the development of approaches making use of physically based models for RWU and isotopic fractionation to analyze experimental data, especially since several soil-vegetation-atmosphere transfer (SVAT) models are available that

20   can simulate flow of isotopologues in the soil and the plant (i.e., SiSPAT-Isotope, Braud et al., 2005; Soil-litter-iso, Haverd and Cuntz, 2010; R-SWMS, Meunier et al., 2017; TOUGHREACT, Singleton et al., 2004; HYDRUS, Sutanto et al., 2012).

To the authors' knowledge, there are only a few studies which attempted to do so. Rothfuss et al. (2012) ran an experiment under controlled laboratory conditions where they measured on four dates (corresponding to four different stages of vegetation and therefore root development) soil water potential and isotopic composition profiles, and root length density

25   distribution profiles. In their experiment, the isotopic composition of transpiration was known. The authors used a global optimization algorithm to obtain the set of parameter of SiSPAT-Isotope that best reflected the experimental dataset. Distributions of RWU could be determined on these four dates. Also, in the study of Mazzacavallo and Kulmatiski (2015), the RWU model of HYDRUS could be parameterized during a labelling (heavy water ^2H_2O) pulse experiment on the basis of measurements of xylem water hydrogen and oxygen isotopic compositions. This provided insights into the existence of niche

30   complementarity between tree (mopane) and grasses species. Note, however, that this HYDRUS version did not incorporate isotopic transport through the soil and the roots.

Another example is the work of Ogle et al. (2004) who could reconstruct active root area and RWU profiles from isotopic measurements using the 1D analytical macroscopic model of Campbell (1991) in a Bayesian framework (root area profile and deconvolution algorithm – RAPID). By assuming normal a priori distributions for the xylem water oxygen and hydrogen isotopic compositions and considering prior knowledge on RWU distribution (i.e., synthetic information based on

5   measurements of other studies), Ogle et al. (2004) obtained a posteriori distributions of x of a desert shrub (Larrea tridentate).

Simple analytical models, such as the formulation of Couvreur et al. (2012), can be applied and confronted with isotopic data. In comparison with statistical tools, such physical models provide profiles with high spatial resolution and lower uncertainty, on the condition that all required (isotopic) data is available. We recognize that in comparison with the statistical

10   and conceptual methodologies presented in this review, using a physical (analytical or numerical) model implies the measurements of additional state variables to be fed as input to the model, and of one parameter (K_{plant}) (when considering the assumption $K_{plant} = K_{comp}$ valid, see Appendix B). Some of these variables are laborious to obtain (e.g., RLD) or not straightforward to measure (H_S, H_L, and T) – especially in the field – but are mandatory to be able to determine contributions to T across a set of identified water sources. In addition, they are necessary to gain insights into soil-plant interactions, e.g.,

15   dynamics of root function (active versus non-active roots in the soil profile) in water uptake and, thus, quantify the disconnection between measured RLD and the prognostic variable SSF (see Appendix B1). For doing this, controlled conditions in state-of-the-art climatic chambers are ideal, as they allow for a reduction of the inherent spatial heterogeneity present under natural conditions and, thus, the deconvolution of environmental effects on RWU. Experimental facilities that not only control atmospheric forcing (soil upper boundary conditions for latent and heat flow), but impose lower boundaries

20   for the soil compartment (e.g., drainage and capillary rise dynamics) and provide means to close the hydrological balance are required. Moreover, macrocosm experiments (~m^3 scale) should be favored over mesocosm (~dm^3 scale) experiments to avoid or reduce inherent side effects that would ultimately hamper mimicking natural conditions.

6 CONCLUSION

Root water uptake is a key process in the global water cycle. More than 50% of total terrestrial evapotranspiration crosses plant roots to go back to the atmosphere (Jasechko et al., 2013). Despite its importance, quantification of RWU remains difficult due to the opaque nature of the soil and the spatial and temporal variability of the uptake process.

5   Water stable isotopic analysis is a powerful and valuable tool for the assessment of plant water sources. In an inverse modelling framework, isotopic analysis of plant tissues and soil also allow for obtaining species-specific parametrization of physically based analytical and numerical RWU models. They provide a unique way to tackle the difficulty of disentangling actual RWU profiles with root traits and characteristics. Yet, our literature review revealed that isotopic data have been up to now mainly used to assess water sources under natural ecosystems using statistical approaches. Only 4% of current scientific

10   publications demonstrate the use of a physically based model for analyzing isotopic data.

Three methods (representing 90% of the studies) have been used for partitioning water sources: the "direct inference" method, the two end-member mixing model and two examples of multi-source mixing models. We performed a comparison between these methods. We could quantify the impact of the definition of the plant water sources (i.e., whether they are spatially disjoint or not and whether their isotopic compositions values are significantly different or not) on the outcome of

15   the two end-member mixing model. We highlighted the importance of systematically reporting uncertainties along with estimates of contribution to T of given plant water sources. The inter-comparison also illustrated the limitations of the graphical inference method and the multi-source mixing model of Phillips and Gregg (2003), whereas it underlined the good performance of the Bayesian approach of (Parnell et al., 2010), which uses a more rigorous statistical framework, if the number of considered water sources matches the number of isotopic measurements in the soil profile. However, contrary to

20   the analytical model none of the graphical and statistical methods could locate and quantify hydraulic redistribution of water. Finally, the authors call for a generalization of coupled approaches relying on the confrontation between labelling experiments under controlled conditions and three dimensional RWU numerical modelling. This type of approach could be used in agronomy and agriculture to quantify root water uptake as a function of plant genotype, soil structure and climate.

REFERENCES

Andrade, J. L., Meinzer, F. C., Goldstein, G., and Schnitzer, S. A.: Water uptake and transport in lianas and co-occurring trees of a seasonally dry tropical forest, Trees-Struct Funct, 19, 282-289, doi: 10.1007/s00468-004-0388-x, 2005.

Araguás-Araguás, L., Rozanski, K., Gonfiantini, R., and Louvat, D.: Isotope effects accompanying vacuum extraction of soil-water for stable-isotope analyses, J. Hydrol., 168, 159-171, doi: 10.1016/0022-1694(94)02636-P, 1995.

Araki, H. and Iijima, M.: Stable isotope analysis of water extraction from subsoil in upland rice (Oryza sativa L.) as affected by drought and soil compaction, Plant Soil, 270, 147-157, doi: 10.1007/s11104-004-1304-2, 2005.

Armas, C., Kim, J. H., Bleby, T. M., and Jackson, R. B.: The effect of hydraulic lift on organic matter decomposition, soil nitrogen cycling, and nitrogen acquisition by a grass species, Oecologia, 168, 11-22, doi: 10.1007/s00442-011-2065-2, 2012.

Asbjornsen, H., Mora, G., and Helmers, M. J.: Variation in water uptake dynamics among contrasting agricultural and native plant communities in the Midwestern US, Agr Ecosyst Environ, 121, 343-356, doi: 10.1016/j.agee.2006.11.009, 2007.

Bachmann, D., Gockele, A., Ravenek, J. M., Roscher, C., Strecker, T., Weigelt, A., and Buchmann, N.: No evidence of complementary water use along a plant species richness gradient in temperate experimental grasslands, Plos One, 10, doi: 10.1371/journal.pone.0116367, 2015.

Bariac, T., Gonzalezdunia, J., Tardieu, F., Tessier, D., and Mariotti, A.: Spatial variation of the isotopic composition of water (O-18, H-2) in organs of aerophytic plants .1. Assessment under Laboratory Conditions, Chem Geol, 115, 307-315, doi: 10.1016/0009-2541(94)90194-5, 1994.

Barnes, C. J. and Allison, G. B.: The distribution of deuterium and O-18 in dry Soils. 1. Theory, J. Hydrol., 60, 141-156, doi: 10.1016/0022-1694(83)90018-5, 1983.

Barthold, F. K., Tyralla, C., Schneider, K., Vache, K. B., Frede, H. G., and Breuer, L.: How many tracers do we need for end member mixing analysis (EMMA)? A sensitivity analysis, Water Resour. Res., 47, doi: 10.1029/2011wr010604, 2011.

Beyer, M., Koeniger, P., Gaj, M., Hamutoko, J. T., Wanke, H., and Himmelsbach, T.: A deuterium-based labeling technique for the investigation of rooting depths, water uptake dynamics and unsaturated zone water transport in semiarid environments, J. Hydrol., 533, 627-643, doi: 10.1016/j.jhydrol.2015.12.037, 2016.

Bijoor, N. S., McCarthy, H. R., Zhang, D. C., and Pataki, D. E.: Water sources of urban trees in the Los Angeles metropolitan area, Urban Ecosyst, 15, 195-214, doi: 10.1007/s11252-011-0196-1, 2012.

Boujamlaoui, Z., Bariac, T., Biron, P., Canale, L., and Richard, P.: Profondeur d'extraction racinaire et signature isotopique de l'eau prélevée par les racines des couverts végétaux, C. R. Geoscience, 337, 589–598, doi: 10.1016/j.crte.2005.02.003, 2005.

Braud, I., Bariac, T., Gaudet, J. P., and Vauclin, M.: SiSPAT-Isotope, a coupled heat, water and stable isotope (HDO and $H_2^{18}O$) transport model for bare soil. Part I. Model description and first verifications, J. Hydrol., 309, 277-300, doi: 10.1016/j.jhydrol.2004.12.013, 2005.

Brunel, J. P., Walker, G. R., and Kennettsmith, A. K.: Field validation of isotopic procedures for determining sources of water used by plants in a semiarid environment, J. Hydrol., 167, 351-368, doi: 10.1016/0022-1694(94)02575-V, 1995.

Caldwell, M. M. and Richards, J. H.: Hydraulic Lift - Water efflux from upper roots improves effectiveness of water-uptake by deep roots, Oecologia, 79, 1-5, doi: 10.1007/Bf00378231, 1989.

Campbell, G. S.: Simulation of water uptake by plant roots. In: Modeling Plant and Soil Systems, Hanks, J. and Ritchie, J. T. (Eds.), American Society of Agronomy, Madison, WI., 1991.

Carminati, A., Kroener, E., and Ahmed, M. A.: Excudation of mucilage (Water for Carbon, Carbon for Water), Vadose Zone J., 15, 2016.

Christophersen, N. and Hooper, R. P.: Multivariate-analysis of stream water chemical-data - the use of principal components-analysis for the end-member mixing problem, Water Resour. Res., 28, 99-107, doi: 10.1029/91wr02518, 1992.

Couvreur, V., Vanderborght, J., Draye, X., and Javaux, M.: Dynamic aspects of soil water availability for isohydric plants: Focus on root hydraulic resistances, Water Resour. Res., 50, doi: 10.1002/2014WR015608, 2014.

Couvreur, V., Vanderborght, J., and Javaux, M.: A simple three-dimensional macroscopic root water uptake model based on the hydraulic architecture approach, Hydrol. Earth Syst. Sc., 16, 2957-2971, doi: 10.5194/hess-16-2957-2012, 2012.

5   Craig, H. and Gordon, L. I.: Deuterium and oxygen 18 variations in the ocean and marine atmosphere, Spoleto, Italy1965, 9-130, 1965.

Dawson, T. E.: Hydraulic lift and water-use by plants - implications for water-balance, performance and plant-plant interactions, Oecologia, 95, 565-574, doi: 10.1007/BF00317442, 1993.

Dawson, T. E. and Ehleringer, J. R.: Isotopic enrichment of water in the woody tissues of plants - Implications for plant water source, water-uptake, and other studies which use the stable isotopic composition of cellulose, Geochim. Cosmochim. Acta, 57, 3487-3492, doi: 10.1016/0016-7037(93)90554-A, 1993.

Dawson, T. E. and Ehleringer, J. R.: Streamside trees that do not use stream water, Nature, 350, 335-337, doi: 10.1038/350335a0, 1991.

Dawson, T. E. and Pate, J. S.: Seasonal water uptake and movement in root systems of Australian phraeatophytic plants of dimorphic root morphology: A stable isotope investigation, Oecologia, 107, 13-20, doi: 10.1007/Bf00582230, 1996.

Ellsworth, P. Z. and Williams, D. G.: Hydrogen isotope fractionation during water uptake by woody xerophytes, Plant Soil, 291, 93-107, doi: 10.1007/s11104-006-9177-1, 2007.

Erhardt, E. B. and Bedrick, E. J.: A Bayesian framework for stable isotope mixing models, Environ. Ecol. Stat., 20, 377-397, doi: 10.1007/s10651-012-0224-1, 2013.

20 Farquhar, G. D., Cernusak, L. A., and Barnes, B.: Heavy water fractionation during transpiration, Plant Physiol., 143, 11-18, 2007.

Feikema, P. M., Morris, J. D., and Connell, L. D.: The water balance and water sources of a Eucalyptus plantation over shallow saline groundwater, Plant Soil, 332, 429-449, doi: 10.1007/s11104-010-0309-2, 2010.

Gaines, K. P., Stanley, J. W., Meinzer, F. C., McCulloh, K. A., Woodruff, D. R., Chen, W., Adams, T. S., Lin, H., and Eissenstat, D. M.: Reliance on shallow soil water in a mixed-hardwood forest in central Pennsylvania, Tree Physiol, 36, 444-458, doi: 10.1093/treephys/tpv113, 2016.

Gaj, M., Beyer, M., Koeniger, P., Wanke, H., Hamutoko, J., and Himmelsbach, T.: In-situ unsaturated zone stable water isotope (^{2}H and ^{18}O) measurements in semi-arid environments using tunable off-axis integrated cavity output spectroscopy, hydrol. Earth Syst. Sci., 20, 715-731, doi: 10.5194/hess-20-715-2016, 2015.

30 Gangi, L., Rothfuss, Y., Ogée, J., Wingate, L., Vereecken, H., and Brüggemann, N.: A new method for in situ measurements of oxygen isotopologues of soil water and carbon dioxide with high time resolution Vadose Zone J., 14, doi: 10.2136/vzj2014.11.0169, 2015.

Goebel, T. S., Lascano, R. J., Paxton, P. R., and Mahan, J. R.: Rainwater use by irrigated cotton measured with stable isotopes of water, Agric. Water Manage., 158, 17-25, doi: 10.1016/j.agwat.2015.04.005, 2015.

35 Gonfiantini, R.: Standards for stable isotope measurements in natural compounds, Nature, 271, 534-536, doi: 10.1038/271534a0, 1978.

Gralher, B., Herbstritt, B., Weiler, M., Wassenaar, L. I., and Stumpp, C.: Correcting Laser-Based Water Stable Isotope Readings Biased by Carrier Gas Changes, Environ. Sci. Technol., 50, 7074-7081, doi: 10.1021/acs.est.6b01124, 2016.

40 Grossiord, C., Gessler, A., Granier, A., Berger, S., Brechet, C., Hentschel, R., Hommel, R., Scherer-Lorenzen, M., and Bonal, D.: Impact of interspecific interactions on the soil water uptake depth in a young temperate mixed species plantation, J. Hydrol., 519, 3511-3519, doi: 10.1016/j.jhydrol.2014.11.011, 2014.

Guderle, M. and Hildebrandt, A.: Using measured soil water contents to estimate evapotranspiration and root water uptake profiles - a comparative study, Hydrol. Earth Syst. Sc., 19, 409-425, doi: 10.5194/hess-19-409-2015, 2015.

45 Hastings, W. K.: Monte-carlo sampling methods using markov chains and their applications, Biometrika, 57, 97-&, doi: 10.2307/2334940, 1970.

Haverd, V. and Cuntz, M.: Soil-Litter-Iso: A one-dimensional model for coupled transport of heat, water and stable isotopes in soil with a litter layer and root extraction, J. Hydrol., 388, 438-455, doi: 10.1016/j.jhydrol.2010.05.029, 2010.

Heinen, M.: Compensation in Root Water Uptake Models Combined with Three-Dimensional Root Length Density Distribution, Vadose Zone J., 13, doi: 10.2136/vzj2013.08.0149, 2014.

Herbstritt, B., Gralher, B., and Weiler, M.: Continuous in situ measurements of stable isotopes in liquid water, Water Resour. Res., 48, doi: 10.1029/2011wr011369, 2012.

Huber, K., Vanderborght, J., Javaux, M., and Vereecken, H.: Simulating transpiration and leaf water relations in response to heterogeneous soil moisture and different stomatal control mechanisms, Plant Soil, 394, 109-126, doi: 10.1007/s11104-015-2502-9, 2015.

Hupet, F., Lambot, S., Javaux, M., and Vanclooster, M.: On the identification of macroscopic root water uptake parameters from soil water content observations, Water Resour. Res., 38, doi: 10.1029/2002wr001556, 2002.

Ingraham, N. L. and Shadel, C.: A comparison of the toluene distillation and vacuum heat methods for extracting soil-water or stable isotopic analysis, J. Hydrol., 140, 371-387, doi: 10.1016/0022-1694(92)90249-U, 1992.

Isaac, M. E., Anglaaere, L. C. N., Borden, K., and Adu-Bredu, S.: Intraspecific root plasticity in agroforestry systems across edaphic conditions, Agr Ecosyst Environ, 185, 16-23, doi: 10.1016/j.agee.2013.12.004, 2014.

Jarvis, N. J.: A simple empirical model of root water uptake, J. Hydrol., 107, 57–72, doi: 10.1016/0022-1694(89)90050-4, 1989.

Jarvis, N. J.: Simple physics-based models of compensatory plant water uptake: concepts and eco-hydrological consequences, Hydrol. Earth Syst. Sc., 15, 3431-3446, doi: 10.5194/hess-15-3431-2011, 2011.

Jasechko, S., Sharp, Z. D., Gibson, J. J., Birks, S. J., Yi, Y., and Fawcett, P. J.: Terrestrial water fluxes dominated by transpiration, Nature, 496, 347-350, doi: 10.1038/Nature11983, 2013.

Javaux, M., Couvreur, V., Vander Borght, J., and Vereecken, H.: Root Water Uptake: From Three-Dimensional Biophysical Processes to Macroscopic Modeling Approaches, Vadose Zone J., 12, doi: 10.2136/vzj2013.02.0042, 2013.

Javaux, M., Rothfuss, Y., Vanderborght, J., Vereecken, H., and Brüggemann, N.: Isotopic composition of plant water sources, Nature, 536, E1-E3, doi: 10.1038/nature18946, 2016.

Koch, P. L. and Phillips, D. L.: Incorporating concentration dependence in stable isotope mixing models: a reply to Robbins, Hilderbrand and Farley (2002), Oecologia, 133, 14-18, doi: 10.1007/s00442-002-0977-6, 2002.

Koeniger, P., Marshall, J. D., Link, T., and Mulch, A.: An inexpensive, fast, and reliable method for vacuum extraction of soil and plant water for stable isotope analyses by mass spectrometry, Rapid Commun. Mass Spectrom., 25, 3041-3048, doi: 10.1002/Rcm.5198, 2011.

Kurz-Besson, C., Otieno, D., do Vale, R. L., Siegwolf, R., Schmidt, M., Herd, A., Nogueira, C., David, T. S., David, J. S., Tenhunen, J., Pereira, J. S., and Chaves, M.: Hydraulic lift in cork oak trees in a savannah-type Mediterranean ecosystem and its contribution to the local water balance, Plant Soil, 282, 361-378, doi: 10.1007/s11104-006-0005-4, 2006.

Leroux, X., Bariac, T., and Mariotti, A.: Spatial partitioning of the soil-water resource between grass and shrub components in a west-African humid savanna, Oecologia, 104, 147-155, doi: 10.1007/BF00328579, 1995.

Li, S. G., Romero-Saltos, H., Tsujimura, M., Sugimoto, A., Sasaki, L., Davaa, G., and Oyunbaatar, D.: Plant water sources in the cold semiarid ecosystem of the upper Kherlen River catchment in Mongolia: A stable isotope approach, J. Hydrol., 333, 109-117, doi: 10.1016/j.jhydrol.2006.07.020, 2007.

Lin, G. H. and Sternberg, L. D. L.: Comparative-study of water-Uptake and photosynthetic gas-exchange between scrub and fringe red mangroves, Rhizophora-Mangle L, Oecologia, 90, 399-403, doi: 10.1007/Bf00317697, 1992.

Mazzacavallo, M. G. and Kulmatiski, A.: Modelling water uptake provides a new perspective on grass and tree coexistence, Plos One, 10, doi: 10.1371/journal.pone.0144300, 2015.

McCole, A. A. and Stern, L. A.: Seasonal water use patterns of Juniperus ashei on the Edwards Plateau, Texas, based on stable isotopes in water, J. Hydrol., 342, 238-248, doi: 10.1016/j.jhydrol.2007.05.024, 2007.

McDonnell, J. J.: The two water worlds hypothesis: ecohydrological separation of water between streams and trees?, WIREs Water, 1, 323–329, doi: 10.1002/wat2.1027, 2014.

Metropolis, N., Rosenbluth, A. W., Rosenbluth, M. N., Teller, A. H., and Teller, E.: Equation of state calculations by fast computing machines, J Chem Phys, 21, 1087-1092, doi: 10.1063/1.1699114, 1953.

Meunier, F., Rothfuss, Y., Bariac, T., Biron, P., Durand, J.-L., Richard, P., Couvreur, V., J, V., and Javaux, M.: Measuring and modeling Hydraulic Lift of *Lolium multiflorum* using stable water isotopes, accepted in Vadose Zone Journal, 2017. 2017.

Midwood, A. J., Boutton, T. W., Archer, S. R., and Watts, S. E.: Water use by woody plants on contrasting soils in a savanna parkland: assessment with δ^2H and δ^{18}O Plant Soil, 205, 13-24, doi: 10.1023/A:1004355423241, 1998.

Moore, J. W. and Semmens, B. X.: Incorporating uncertainty and prior information into stable isotope mixing models, Ecol. Lett., 11, 470-480, doi: 10.1111/j.1461-0248.2008.01163.x, 2008.

Moreira, M. Z., Sternberg, L. D. L., and Nepstad, D. C.: Vertical patterns of soil water uptake by plants in a primary forest and an abandoned pasture in the eastern Amazon: an isotopic approach, Plant Soil, 222, 95-107, doi: 10.1023/A:1004773217189, 2000.

Musters, P. A. D. and Bouten, W.: Assessing rooting depths of an Austrian pine stand by inverse modeling soil water content maps, Water Resour. Res., 35, 3041-3048, doi: 10.1029/1999wr900173, 1999.

Musters, P. A. D. and Bouten, W.: A method for identifying optimum strategies of measuring soil water contents for calibrating a root water uptake model, J. Hydrol., 227, 273-286, doi: 10.1016/S0022-1694(99)00187-0, 2000.

Nadezhdina, N., David, T. S., David, J. S., Ferreira, M. I., Dohnal, M., Tesar, M., Gartner, K., Leitgeb, E., Nadezhdin, V., Cermak, J., Jimenez, M. S., and Morales, D.: Trees never rest: the multiple facets of hydraulic redistribution, Ecohydrology, 3, 431-444, doi: 10.1002/eco.148, 2010.

Nadezhdina, N., David, T. S., David, J. S., Nadezhdin, V., Cermak, J., Gebauer, R., Ferreira, M. I., Conceicao, N., Dohnal, M., Tesar, M., Gartner, K., and Ceulemans, R.: Root Function: In Situ Studies Through Sap Flow Research, Measuring Roots: An Updated Approach, doi: 10.1007/978-3-642-22067-8_14, 2012. 267-290, doi: 10.1007/978-3-642-22067-8_14, 2012.

Nadezhdina, N., Ferreira, M. I., Conceicao, N., Pacheco, C. A., Hausler, M., and David, T. S.: Water uptake and hydraulic redistribution under a seasonal climate: long-term study in a rainfed olive orchard, Ecohydrology, 8, 387-397, doi: 10.1002/eco.1545, 2015.

Oerter, E., Finstad, K., Schaefer, J., Goldsmith, G. R., Dawson, T., and Amundson, R.: Oxygen isotope fractionation effects in soil water via interaction with cations (Mg, Ca, K, Na) adsorbed to phyllosilicate clay minerals, J. Hydrol., 515, 1-9, doi: 10.1016/j.jhydrol.2014.04.029, 2014.

Oerter, E. J., Perelet, A., Pardyjak, E., and Bowen, G.: Membrane inlet laser spectroscopy to measure H and O stable isotope compositions of soil and sediment pore water with high sample throughput, Rapid Commun Mass Spectrom, doi: 10.1002/rcm.7768, 2016. doi: 10.1002/rcm.7768, 2016.

Ogle, K., Tucker, C., and Cable, J. M.: Beyond simple linear mixing models: process-based isotope partitioning of ecological processes, Ecol. Appl., 24, 181-195, doi: 10.1890/1051-0761-24.1.181, 2014.

Ogle, K., Wolpert, R. L., and Reynolds, J. F.: Reconstructing plant root area and water uptake profiles, Ecology, 85, 1967-1978, doi: 10.1890/03-0346, 2004.

Orlowski, N., Breuer, L., and McDonnell, J. J.: Critical issues with cryogenic extraction of soil water for stable isotope analysis, Ecohydrology, 9, 3-10, doi: 10.1002/eco.1722, 2016a.

Orlowski, N., Frede, H.-G., Brüggemann, N., and Breuer, L.: Validation and application of a cryogenic vacuum extraction system for soil and plant water extraction for isotope analysis, J. Sens. Sens. Syst., 2, 179–193, doi: 10.5194/jsss-2-179-2013, 2013.

Orlowski, N., Pratt, D. L., and McDonnell, J. J.: Intercomparison of soil pore water extraction methods for stable isotope analysis, Hydrol. Process., 30, 3434-3449, doi: 10.1002/hyp.10870, 2016b.

Parnell, A. C., Inger, R., Bearhop, S., and Jackson, A. L.: Source partitioning using stable isotopes: coping with too much variation, Plos One, 5, e9672, doi: 10.1371/journal.pone.0009672, 2010.

Parnell, A. C., Phillips, D. L., Bearhop, S., Semmens, B. X., Ward, E. J., Moore, J. W., Jackson, A. L., Grey, J., Kelly, D. J., and Inger, R.: Bayesian stable isotope mixing models, Environmetrics, 24, 387–399, doi: 10.1002/env.2221, 2013.

Phillips, D. L. and Gregg, J. W.: Source partitioning using stable isotopes: Coping with too many sources, Oecologia, 136, 261-269, doi: 10.1007/s00442-003-1218-3, 2003.

Phillips, D. L. and Gregg, J. W.: Uncertainty in source partitioning using stable isotopes, Oecologia, 127, 171-179, doi: 10.1007/s004420000578, 2001.

Phillips, D. L. and Koch, P. L.: Incorporating concentration dependence in stable isotope mixing models, Oecologia, 130, 114-125, doi: 10.1007/s004420100786, 2002.

Phillips, D. L., Newsome, S. D., and Gregg, J. W.: Combining sources in stable isotope mixing models: alternative methods, Oecologia, 144, 520-527, doi: 10.1007/s00442-004-1816-8, 2005.

Pratt, D. L., Lu, M., Barbour, S. L., and Hendry, M. J.: An evaluation of materials and methods for vapour measurement of the isotopic composition of pore water in deep, unsaturated zones, Isotopes Environ. Health Stud., doi: 10.1080/10256016.2016.1151423, 2016. doi: 10.1080/10256016.2016.1151423, 2016.

Prechsl, U. E., Burri, S., Gilgen, A. K., Kahmen, A., and Buchmann, N.: No shift to a deeper water uptake depth in response to summer drought of two lowland and sub-alpine C$_3$-grasslands in Switzerland, Oecologia, 177, 97-111, doi: 10.1007/s00442-014-3092-6, 2015.

Romero-Saltos, H., Sternberg Lda, S., Moreira, M. Z., and Nepstad, D. C.: Rainfall exclusion in an eastern Amazonian forest alters soil water movement and depth of water uptake, Am. J. Bot., 92, 443-455, doi: 10.3732/ajb.92.3.443, 2005.

Rossatto, D. R., Sternberg, L. D. L., and Franco, A. C.: The partitioning of water uptake between growth forms in a Neotropical savanna: do herbs exploit a third water source niche?, Plant Biol., 15, 84-92, doi: 10.1111/j.1438-8677.2012.00618.x, 2013.

Rothfuss, Y., Biron, P., Braud, I., Canale, L., Durand, J. L., Gaudet, J. P., Richard, P., Vauclin, M., and Bariac, T.: Partitioning evapotranspiration fluxes into soil evaporation and plant transpiration using water stable isotopes under controlled conditions, Hydrol. Process., 24, 3177-3194, doi: 10.1002/Hyp.7743, 2010.

Rothfuss, Y., Braud, I., Le Moine, N., Biron, P., Durand, J. L., Vauclin, M., and Bariac, T.: Factors controlling the isotopic partitioning between soil evaporation and plant transpiration: Assessment using a multi-objective calibration of SiSPAT-Isotope under controlled conditions, J. Hydrol., 442, 75-88, doi: 10.1016/j.jhydrol.2012.03.041, 2012.

Rothfuss, Y., Merz, S., Vanderborght, J., Hermes, N., Weuthen, A., Pohlmeier, A., Vereecken, H., and Brüggemann, N.: Long-term and high frequency non-destructive monitoring of water stable isotope profiles in an evaporating soil column, Hydrol. Earth Syst. Sci., 19, 4067-4080, doi: 10.5194/hess-19-4067-2015, 2015.

Rothfuss, Y., Vereecken, H., and Brüggemann, N.: Monitoring water stable isotopic composition in soils using gas-permeable tubing and infrared laser absorption spectroscopy, Water Resour. Res., 49, 1-9, doi: 10.1002/wrcr.20311, 2013.

Roupsard, O., Ferhi, A., Granier, A., Pallo, F., Depommier, D., Mallet, B., Joly, H. I., and Dreyer, E.: Reverse phenology and dry-season water uptake by Faidherbia albida (Del.) A. Chev. in an agroforestry parkland of Sudanese west Africa, Funct. Ecol., 13, 460-472, doi: 10.1046/j.1365-2435.1999.00345.x, 1999.

Sánchez-Perez, J. M., Lucot, E., Bariac, T., and Tremolieres, M.: Water uptake by trees in a riparian hardwood forest (Rhine floodplain, France), Hydrol. Process., 22, 366-375, doi: 10.1002/hyp.6604, 2008.

Scheenen, T. W. J., van Dusschoten, D., de Jager, P. A., and Van As, H.: Quantification of water transport in plants with NMR imaging, J. Exp. Bot., 51, 1751-1759, doi: 10.1093/jexbot/51.351.1751, 2000.

Schwendenmann, L., Pendall, E., Sanchez-Bragado, R., Kunert, N., and Holscher, D.: Tree water uptake in a tropical plantation varying in tree diversity: interspecific differences, seasonal shifts and complementarity, Ecohydrology, 8, 1-12, doi: 10.1002/eco.1479, 2015.

Simunek, J. and Hopmans, J. W.: Modeling compensated root water and nutrient uptake, Ecol. Model., 220, 505-521, doi: 10.1016/j.ecolmodel.2008.11.004, 2009.

Singleton, M. J., Sonnenthal, E. L., Conrad, M. E., DePaolo, D. J., and Gee, G. W.: Multiphase reactive transport modeling of seasonal infiltration events and stable isotope fractionation in unsaturated zone pore water and vapor at the Hanford site, Vadose Zone J., 3, 775-785, doi: 10.2136/vzj2004.0775, 2004.

Sofer, Z. and Gat, J. R.: Activities and concentrations of oxygen-18 in concentrated aqueous salt solutions - analytical and geophysical implications, Earth Planet. Sc. Lett., 15, 232-&, doi: 10.1016/0012-821x(72)90168-9, 1972.

Sprenger, M., Herbstritt, B., and Weiler, M.: Established methods and new opportunities for pore water stable isotope analysis, Hydrol. Process., doi: 10.1002/hyp.10643, 2015. doi: 10.1002/hyp.10643, 2015.

Sprenger, M., Leistert, H., Gimbel, K., and Weiler, M.: Illuminating hydrological processes at the soil-vegetation-atmosphere interface with water stable isotopes, Review of Geophysics, 54, 674-704, doi: 10.1002/2015RG000515, 2016.

Stahl, C., Herault, B., Rossi, V., Burban, B., Brechet, C., and Bonal, D.: Depth of soil water uptake by tropical rainforest trees during dry periods: does tree dimension matter?, Oecologia, 173, 1191-1201, doi: 10.1007/s00442-013-2724-6, 2013.

Stumpp, C., Stichler, W., Kandolf, M., and Simunek, J.: Effects of Land Cover and Fertilization Method on Water Flow and Solute Transport in Five Lysimeters: A Long-Term Study Using Stable Water Isotopes, Vadose Zone J., 11, doi: 10.2136/vzj2011.0075, 2012.

Sutanto, S. J., Wenninger, J., Coenders-Gerrits, A. M. J., and Uhlenbrook, S.: Partitioning of evaporation into transpiration, soil evaporation and interception: a comparison between isotope measurements and a HYDRUS-1D model, Hydrol. Earth Syst. Sci., 16, 2605-2616, doi: 10.5194/hess-16-2605-2012, 2012.

Tardieu, F. and Davies, W. J.: Integration of Hydraulic and Chemical Signaling in the Control of Stomatal Conductance and Water Status of Droughted Plants, Plant Cell Environ, 16, 341-349, doi: 10.1111/j.1365-3040.1993.tb00880.x, 1993.

Thorburn, P. J. and Ehleringer, J. R.: Root water uptake of field-growing plants indicated by measurements of natural-abundance deuterium, Plant Soil, 177, 225-233, doi: 10.1007/Bf00010129, 1995.

Thorburn, P. J., Walker, G. R., and Brunel, J. P.: Extraction of water from eucalyptus trees for analysis of deuterium and O-18 - laboratory and field techniques, Plant Cell Environ, 16, 269-277, doi: 10.1111/j.1365-3040.1993.tb00869.x, 1993.

van Genuchten, M. T.: A closed-form equation for predicting the hydraulic conductivity of unsaturated soils, Soil Sci. Soc. Am. J., 44, 892-898, doi: 10.2136/sssaj1980.03615995004400050002x, 1980.

Vanderklift, M. A. and Ponsard, S.: Sources of variation in consumer-diet δ^{15}N enrichment: a meta-analysis, Oecologia, 136, 169-182, doi: 10.1007/s00442-003-1270-z, 2003.

Vandoorne, B., Beff, L., Lutts, S., and Javaux, M.: Root water uptake dynamics of Cichorium intybus var. sativum under water-limited conditions, Vadose Zone J., 11, doi: 10.2136/vzj2012.0005, 2012.

Volkmann, T. H., Kühnhammer, K., Herbstritt, B., Gessler, A., and Weiler, M.: A method for in situ monitoring of the isotope composition of tree xylem water using laser spectroscopy, Plant Cell Environ, doi: 10.1111/pce.12725, 2016a. doi: 10.1111/pce.12725, 2016a.

Volkmann, T. H. M., Haberer, K., Gessler, A., and Weiler, M.: High-resolution isotope measurements resolve rapid ecohydrological dynamics at the soil–plant interface, New Phytol., doi: 10.1111/nph.13868, 2016b. doi: 10.1111/nph.13868, 2016b.

Volkmann, T. H. M. and Weiler, M.: Continual in situ monitoring of pore water stable isotopes in the subsurface, Hydrol. Earth Syst. Sci., 18, 1819-1833, doi: 10.5194/hess-18-1819-2014, 2014.

Walker, C. D. and Richardson, S. B.: The use of stable isotopes of water in characterizing the source of water in vegetation, Chem Geol, 94, 145-158, doi: 10.1016/0168-9622(91)90007-J, 1991.

Wang, P., Song, X. F., Han, D. M., Zhang, Y. H., and Liu, X.: A study of root water uptake of crops indicated by hydrogen and oxygen stable isotopes: A case in Shanxi Province, China, Agric. Water Manage., 97, 475-482, doi: 10.1016/j.agwat.2009.11.008, 2010.

Washburn, E. W. and Smith, E. R.: The isotopic fractionation of water by physiological processes, Science, 79, 188-189, doi: 10.1126/science.79.2043.188, 1934.

Weltzin, J. F. and McPherson, G. R.: Spatial and temporal soil moisture resource partitioning by trees and grasses in a temperate savanna, Arizona, USA, Oecologia, 112, 156-164, doi: 10.1007/s004420050295, 1997.

West, A. G., Patrickson, S. J., and Ehleringer, J. R.: Water extraction times for plant and soil materials used in stable isotope analysis, Rapid Commun. Mass Spectrom., 20, 1317-1321, doi: 10.1002/rcm.2456, 2006.

White, J. W. C., Cook, E. R., Lawrence, J. R., and Broecker, W. S.: The D/H ratios of sap in trees - implications for water sources and tree-Ring D/H ratios, Geochim. Cosmochim. Acta, 49, 237-246, doi: 10.1016/0016-7037(85)90207-8, 1985.

Zarebanadkouki, M., Kim, Y. X., Moradi, A. B., Vogel, H. J., Kaestner, A., and Carminati, A.: Quantification and modeling of local root water uptake using neutron radiography and deuterated water, Vadose Zone J., 11, doi: 10.2136/vzj2011.0196, 2012.

Zimmermann, U., Ehhalt, D., and Münnich, K. O.: Soil water movement and evapotranspiration: changes in the isotopic composition of the water, Vienna1967, 567–584.

AUTHOR CONTRIBUTION

Y. Rothfuss reviewed the published literature. Y. Rothfuss and M. Javaux designed the virtual experiments, analysed, and discussed the obtained results.

ACKNOWLEDGEMENTS

5   This study was conducted in the framework of and with means from the Bioeconomy Portfolio Theme of the Helmholtz Association of German Research Centers. The authors would like to thank Harry Vereecken, Jan Vanderborght, and Nicolas Brüggemann for their insightful comments on the manuscript.

Table 1

Table 1: Summary of the reviewed studies that use one of either the three methods (graphical inference), two-end members mixing model, and "multi-source mixing models) for plant water sources partitioning.

Authors	Experimental conditions (field: F / laboratory: L)
Graphical inference	
Leroux et al., 1995	F (tropical)
Thorburn and Ehleringer, 1995	F (semi-arid; cold desert, subhumid)
Weltzin and McPherson, 1997	F (temperate semi-arid savanna)
Jackson et al., 2009	F (tropical forest / savanna)
Moreira et al., 2000	F (eastern Amazon)
Chimner and Cooper, 2004	F (desert)
Kulmatiski et al., 2006	F (shrub-steppe)
Li et al., 2007	F (cold continental-semiarid)
Wang et al., 2010	F (warm temperate / monsoon climate)
Stahl et al., 2013	F (tropical)
Two-end members mixing model	
White et al., 1985	F (temperate)
Dawson and Ehleringer, 1991	F (riparian zone)
Brunel et al., 1995	F (aeolian sand dune)
Dawson and Pate, 1996	F (mediterranean)
McCole and Stern, 2007	Field conditions (subtropical)
Goebel et al., 2015	F (semi-arid)
Multi-source mixing model	
Asbjornsen et al., 2007	F (cornfield, prairie, oak savanna, and woodland)
Wang et al., 2010	F (warm temperate / monsoon climate)
Huang and Zhang, 2015	F (desert)
Prechsl et al., 2015	F (temperate)
Volkmann et al., 2016	F (temperate)

Plant species
Hyparrhenia diplandra, Andropogon schirensis, Imperata cylindrica (grasses), *Cussonia barteri, Crossopteryx febrifuga, Bridelia ferruginea* (shrubs)
Eucalyptus largiflorens, camaldulensis, Acer negundo and grandidentatum, Atriplex canescens, Chrysothamnus, nauseosus, Vanclevea stylosa
Quercus emoryi Torr., Trachypogon montufari (H.B.K.) Nees. (deciduous) *Qualea grandiflora Mart., Q. parviflora Mart., Kielmeyera coriacea (Spr.) Mart., Pterodon pubescens Benth., Dalbergia myscolobium Benth. /* (evergreen) *Didymopanax macrocarpum, Sclerolobium paniculatum, Miconia ferruginata, Roupala montana*
(invasive) *Solanum crinitum Lamb.* (native) *Panicum maximum Jacq.*
Sarcobatus vermiculatus, Chrysothamnus nauseosus, and Chrysothamnus greenei
(invasive) *Centaurea diffusa,* (native) *Pseudoroegneria spicata; Bromus tectorum L.*
Larix sibirica
Summer corn and cotton (species not specified)
tropical rainforest trees
Taxodium distichum / Pinus strobus
Acer grandidentatum Nutt., A negundo L., Quercus gambelii Nutt.
"Mallee Tree" *(Eucalyptus sp.)*
Banksia prionotes, Dryandra sessilis, Grevillea (species unknown)
Juniperus ashei
Gossypium hirsutum L.
Quercus macrocarpa, Umus americana L. (trees), *Zea mays L.* (crop), and *Andropogon gerardii* (grass)
Summer corn and cotton (species not specified)
Caragana korshinskii and Artemisia ordosica
Phleum pratense, Lolium multiflorum, Poa pratensis, Taraxacum officinale, Trifolium repens, Rumex obtusifolius, Trisetum flavescens, Phleum rhaeticum, Carum carvi, and Achillea millefolium, Rumex alpestris, Taraxacum officinale and Trifolium, pratense. Quercus petraea and Fagus sylvatica

SAMPLES FOR ISOTOPIC MEASUREMENTS

Soil profile (soil depth: SD [m] / increment: I [m] / number of profiles: Nps / Replicates)	Roots profile (soil depth: SD [m] / increment: I [m] / number of profiles: Npr)
0.10 < SD < 2.00 / 0.01 < I < 0.10 / R = 3	SD = 1.80 / I = 0.10 / R = 16
No profiles, but soil directly surrounding roots are sampled; SD = 1.50 / I = 0.05 / 3 < R < 4	No profiles, but single roots sampled after excavation
SD = 5.00 (depending on the site) R = 2 / 0.05 < I < 0.20	none
4 < SD < 6 / 0.05 < I < 2.00	none
(1st campaign) SD = 0.6 / I = 0.10 / R= 2 at each site / 4 < Nps (per site) < 6 / (2nd campaign) SD = 2.1 / 0.2 < I < 0.30 / Nps = 10	SD = 4 / 0.25 < I < 0.50 / R = 3
1.05 < SD < 2.20 / 0.10 < I < 0.60	none (reference made to Cooper and Chimner, unpublished data)
SD = 1.00 / 0.05 < I < 0.30	1.20 < SD < 2.20 / I = 0.15
SD = 1.50 / 0.05 < I < 0.30 / Nps = 7	none
SD = 2.00 / 0.20 < I < 0.30 / R = 6	none
none	none (reference made to other literature)
SD = 0.50	none
50 < SD < 4.2 / 0.10 < I < 0.25	none
none (sand around the root system)	none
SD = 0.30 / 0.05 < I < 0.10 / 4 < Nps (per site) < 5	none (qualitative observation)
SD = 0.3 / I ~ 0.02 / Nps = 4 per irrigation treatment	none (reference made to other literature)
1.40 < SD < 2.00 / 0.05 < I < 0.20 / R=2 per site	none
SD = 1.50 / 0.05 < I < 0.30 / Nps = 7	none
SD = 2.00 / 0.05 < I < 0.50	none
0.30 < SD < 0.40 / 0.04 < I < 0.10 / R = 3	SD = 0.30 / 0.075 < I < 0.125 / 6 < Npr < 7
SD = 0.60 / 0.05 < I < 0.10 / Nps > 17	SD = 0.60 / 0.05 < I < 0.10 / R = 4

Natural Abundance: NAb / labelling Experiment: LE	Water extraction method (cryogenic vacuum distillation: Cr / azeotropic distillation Az / direct equilibration: GI / mild vacuum distillation: Mi)	Plant (organ: O / number of samples: Ns / replicates: R / temporal resolution: TR [hrs])
Nab	Cr	O: sapwood trunks (shrub), Crown (grasses) / 8 < Ns < 24 / 0.5 < TR < 1
Nab	Cr / Az	O: non-green, suberised stems / Ns = 3
Nab	Cr	O: stem with phloem tissue / R = 4 (tree and sapling) / O: stem without green tissue / R = 4 (seedling) / O: culm base with sheaths removed / 3 < R < 4
Nab	Cr	O: wood or suberized, mature, stem segments (outer bark and phloem are removed) / R = 2
LE	Cr	O: well suberized stems (trees) / thick fleshy culms covered with dry leaves (grass) / 3 < R < 5
Nab	Cr	O: fully suberized stem sections from the base of plants / (1st campaign, S. Vermiculatus) 4 < Ns (per site) < 8 / R = 3 / (1st campaign, C. nauseosus) 5 < Ns (per site) < 6 / R = 3 / (2nd campaign) 3 < Ns < 5 (depending on the species)
Nab	Cr	O: stem
Nab	Cr	O: stem / Ns (per sampling date) = 5
Nab	Cr	O: stems (epidermis contacted with air was removed) / Ns = 7 / TR = 1 per vegetation stage
LE	Cr	O: branch (length = 0.07 m; diameter = 0.1 – 0.3 m). Bark tissue is immediately removed
Nab	none (Sap flow water)	O: wood samples taken at breast height
Nab	Cr	O: mature suberized stems
Nab	Az	O: twigs (bark is removed) / R = 2
Nab	Mi	O: roots, trunks, stem base
Nab	Cr	O: stem
Nab	Cr	O: meristematic petiole reduced in size to 5mm. / 14 < Ns < 17 (depending on the irragtion treatment) / R = 2 / TR = 1
Nab	Di	O: stem (trees); aerial nodal roots just above the soil surface (Zea mays L.); stem (grass) / Ns = 2 per specie
Nab	Cr	O: stems (epidermis contacted with air was removed) / Ns = 7 / TR = 1 per vegetation stage
Nab	Cr	O: twigs (1–2 cm of stem with bark immediately removed) / R = 3
NAb	Cr	O: root crown / 2 < Ns < 10
LE	none	none (measurement of transpiration isotopic composition)

Single: S / Dual: D / "Double Single": DS isotope approach
S (δ^{18}O)
S (δ^{2}H)
D
S (δ^{2}H)
S (δ^{2}H)
S (δ^{18}O)
DS
DS
DS
D
S (δ^{2}H)
S (δ^{2}H)
D
S (δ^{2}H)
S (δ^{18}O)
S (δ^{18}O)
S (δ^{18}O)
DS
DS
DS
S (δ^{2}H)

Main results (RWU depth: z_{RWU} [m] / soil depth z [m] / fraction of *transpiration: x* / Source: So)

$0.00 < z_{RWU} < 0.05$ (grasses, early morning) / $0.05 < z_{RWU} < 0.10$ (grasses, midday) / $z_{RWU} = 0.30$ or $z_{RWU} > 1.50$ (shrubs, no unique solution)

Dominant source: groundwater (Mountain and floodplain) / $0.3 < z_{RWU} < 0.4$ (cold desert)

$z_{RWU} > 0.50$ (trees and sapling) / $z_{RWU} < 0.15$ (2-months-old seedling) / $0.20 < z_{RWU} < 0.35$ (1- and 2-year-old seedlings and grasses)

$z_{RWU} < 2.00$ (four evergreen and one deciduous species) / $z_{RWU} > 2.00$ (three deciduous and one evergreen species)

Fraction of root water uptake from the labeled region $x = 0.20$ (Solanum crinitum Lamb.) $z_{RWU} < 1.00$ (P. maximum Jacq.)

$0.00 < z_{RWU} < 0.50$ (C. nauseosus, pre-monsoon and monsoon periods) / (S. vermiculatus and C. nauseosus) dominant source: groundwater (pre-monsoon period) and switched to precipitation recharged water ($0.30 < z_{RWU} < 0.40$, during mansoon).

$z_{RWU} = 0.15$ (Bromus tectorum L., early season) / $z_{RWU} = 1.20$ (Centaurea diffusa Lam, late season)

$0.10 < z_{RWU} < 0.40$ from $\delta^{18}O$ meas / $0 < z_{RWU} < 0.80$ from $\delta^{2}H$ meas $z_{RWU} = 0.10$ (Corn, jointing stage) / $z_{RWU} = 0.50$ (Corn, flowering stage) /

$z_{RWU} = 0.10$ (Corn, full ripe stage) / $z_{RWU} = 0.40$ (Cotton, seedling stage) / $z_{RWU} = 0.50$ (Cotton, bud stage) / $z_{RWU} = 1.10$ (Cotton, bolls open stage)

$z_{RWU} > 1.00$ (dry periods, tall trees) / More diffuse z_{RWU} for shorter trees

Groundwater: $0.46 < x < 0.64$ wet site) / $0.16 < x < 0.25$ (intermediate site)

So: Groundwater (streamside mature trees) / So: stream water (younger non-streamside trees) / So: Precipitation (younger streamside trees)

$0 < z_{RWU} < 0.4$ with $0.7 < x < 0.9$ (1st site) / $0 < z_{RWU} < 1.5$ with $x = 0.07$ (2nd site)

So: deeper soil layers (dry season) / So: shallow soil layers (wet season)

$z_{RWU} > 0.30$ m (hot, dry summer) / $0.10 < z_{RWU} < 0.30$

Evidence for shifting to rainwater predominantly

$0.0 < z_{RWU} < 0.20$ m with $x < 45\%$ and $x < 36\%$ (crop and grass, resp.) / $0.00 < z_{RWU} < 0.20$ m with $x < 40\%$ and $x < 20\%$ and $z_{RWU} > 0.60$ m with $x < 60\%$ and $x < 80\%$ (Q. macrocarpa and U. americana L., resp.)

$0< z_{RWU} < 0.20$ with $96 < x < 99$ (Corn, jointing stage) / $0.20 < z_{RWU} < 0.50$ cm with $58 < x < 85$ (Corn, flowering stage), $0.00 < z_{RWU} < 0.20$ with $69 < x < 76$ (Corn, full ripe stage) // $0.00 < z_{RWU} < 0.20$ with $27 < x < 49$ (Cotton, seedling stage), $0.20 < z_{RWU} < 0.50$ cm with $79 < x < 84$ (Cotton, bud stage) / $0.50 < z_{RWU} < 0.90$ with $30 < x < 92$ (Cotton, blooming stage) / $z_{RWU} > 90$ cm with $69 < x < 92$ (Cotton, boll open stage)

$0.1< z_{RWU} < 1.0$ (wet seasons) / z_{RWU} not affected by small rainfall events / $z_{RWU} > 1.00$ with x observed to increase from 2 (± 0.7) to 10 (± 1.4)% for both plants after large rainfall event.

$0 < z_{RWU} < 0.10$ with $0.43 < x < 0.68$ (Drought treatment) / $0 < z_{RWU} < 0.10$ with $0.04 < x < 0.37$ and $0.20 < z_{RWU} < 0.35$ with $0.29 < x < 0.48$ (control treatment)

constant RWU depth profile with $0.15 < x < 0.18$ (beech) / $x < 0.15$ for $z < 0.20$ and $0.15 < x < 0.25$ for $z > 0.30$ (beech/oak mixture and oak monoculture)

1   **Table 2**

SOIL DATA	Shallow groundwater table (Sh)						Deep groundwater table (De)						RLD (cm cm⁻³)
z (m)	Dry surface conditions (ShDr)			Wet surface conditions (ShWe)			Dry surface conditions (DeDr)			Wet surface conditions (DeWe)			
	θ (cm³ cm⁻³)	H_S (cm)	δ_S (‰)	θ (cm³ cm⁻³)	H_S (cm)	δ_S (‰)	θ (cm³ cm⁻³)	H_S (cm)	δ_S (‰)	θ (cm³ cm⁻³)	H_S (cm)	δ_S (‰)	
-0.01	0.235	-454	5	0.372	-2	-7	0.044	-9875	11	0.372	-51	-5	6.0
-0.03	0.325	-267	3	0.372	-8	-6	0.055	-3581	7	0.371	-77	-5,5	3.0
-0.07	0.347	-215	1	0.372	-11	-5	0.081	-1661	1	0.372	-14	-7	2.0
-0.15	0.360	-179	-4	0.372	-70	-6	0.105	-1165	-3,5	0.135	-869	-3,5	0.8
-0.30	0.367	-155	-6	0.370	-125	-6,5	0.122	-989	-4	0.134	-889	-4	0.5
-0.50	0.371	-135	-7	0.371	-135	-7	0.165	-730	-5	0.165	-730	-5	0.4
-1.00	0.372	-125	-7	0.372	-125	-7	0.210	-620	-6	0.210	-620	-6	0.3
-2.00	0.372	-125	-7	0.372	-15	-7	0.259	-600	-7	0.259	-600	-7	0.2
PLANT DATA	T (mm h⁻¹)	H_L (cm)		T (mm h⁻¹)	H_L (cm)		T (mm h⁻¹)	H_L (cm)		T (mm h⁻¹)	H_L (cm)		
IT	0.01	-587		0.01	-491		0.01	-2347		0.01	-918		
hT	0.30	-12330		0.30	-12234		0.30	-14090		0.30	-12661		

Table 2: Soil, plant, and isotopic synthetic input data for the different modelling approaches (depth (z) profiles of soil water content θ, total soil water potential H_S, soil water oxygen isotopic composition δ_S, root length density RLD, transpiration rate T, and leaf water potential H_L) "collected" during eight virtual experiments differing in the depth of the groundwater table (Shallow –Sh / Deep – De) and the water status at the soil surface (Dry – Dr / Wet – We).

Table 3

Soil layer r (m)	Shallow groundwater table (Sh)							
	Dry surface conditions (ShDr)				Wet surface conditions (ShWe)			
	Low T (ShDr_lT)		High T (ShDr_hT)		Low T (ShWe_lT)		High T (ShWe_hT)	
	x_{SIAR} mfv(range) (%)	x_{Couv} (1sd) (%)	x_{SIAR} mfv(range) (%)	x_{Couv} (1sd) (%)	x_{SIAR} mfv(range) (%)	x_{Couv} (1sd) (%)	x_{SIAR} mfv(range) (%)	x_{Couv} (1sd) (%)
0-0.02	1(0-35)	5(1)	6(0-37)	11(1)	18(0-48)	13(1)	16(0-53)	11(1)
0.02-0.05	1(0-35)	7(1)	5(0-38)	9(1)	13(0-42)	10(1)	7(0-43)	9(1)
0.05-0.11	3(0-41)	11(1)	10(0-48)	11(1)	11(0-41)	13(1)	7(0-41)	11(1)
0.11-0.225	15(0-57)	10(1)	14(0-47)	10(1)	11(0-46)	10(1)	3(0-43)	10(1)
0.225-0.4	19(0-57)	11(0)	16(0-55)	10(0)	16(0-53)	9(0)	16(0-49)	10(0)
0.4-0.75	16(0-55)	16(0)	17(0-48)	14(0)	18(0-44)	13(1)	15(0-48)	14(0)
0.75-1.5	17(0-52)	27(2)	18(0-46)	23(2)	16(0-48)	21(2)	16(0-53)	23(2)
1.5-2	17(0-59)	14(2)	17(0-47)	12(2)	15(0-52)	11(2)	16(0-51)	12(2)

Soil layer r (m)	Deep groundwater table (De)							
	Dry surface conditions (DeDr)				Wet surface conditions (DeWe)			
	Low T (DeDr_lT)		High T (DeDr_hT)		Low T (DeWe_lT)		High T (DeWe_hT)	
	x_{SIAR} mfv(range) (%)	x_{Couv} (1sd) (%)	x_{SIAR} mfv(range) (%)	x_{Couv} (1sd) (%)	x_{SIAR} mfv(range) (%)	x_{Couv} (1sd) (%)	x_{SIAR} mfv(range) (%)	x_{Couv} (1sd) (%)
0-0.02	1(0-42)	-170(16)	1(0-41)	5(1)	2(0-49)	24(2)	10(0-52)	11(1)
0.02-0.05	1(0-42)	-17(1)	2(0-45)	8(1)	17(0-55)	18(2)	13(0-54)	9(1)
0.05-0.11	1(0-44)	19(6)	5(0-47)	12(1)	16(0-58)	21(2)	16(0-51)	12(1)
0.11-0.225	3(0-55)	28(5)	11(0-51)	10(1)	1(0-39)	3(0)	12(0-43)	12(1)
0.225-0.4	7(0-75)	33(4)	17(0-51)	11(0)	0,8(0-38)	1(0)	9(0-38)	10(0)
0.4-0.75	15(0-68)	57(3)	17(0-56)	16(0)	5(0-46)	7(1)	15(0-53)	14(0)
0.75-1.5	16(0-74)	98(1)	16(0-54)	26(2)	16(0-51)	17(2)	16(0-45)	23(2)
1.5-2	17(0-76)	51(4)	18(0-53)	13(2)	18(0-53)	9(2)	16(0-46)	12(2)

Table 3: Most frequent value (mfv) and range of the density distribution curve of the relative contribution to transpiration across eight defined soil layers as determined by the Bayesian method of Parnell et al. (2010) (x_{SIAR}, %) and mean relative contribution (with standard deviation) provided by the analytical model of Couvreur et al. (2012) (x_{Couv}, %). Profiles of relative contribution were computed for eight soil-plant virtual experiments differing in the depth of the groundwater table (shallow – Sh / deep –De), the soil surface water status (dry – Dr / wet – We), and the plant transpiration rate (low – lT / high – hT).

1   **FIGURES**

2   **Figure 1**
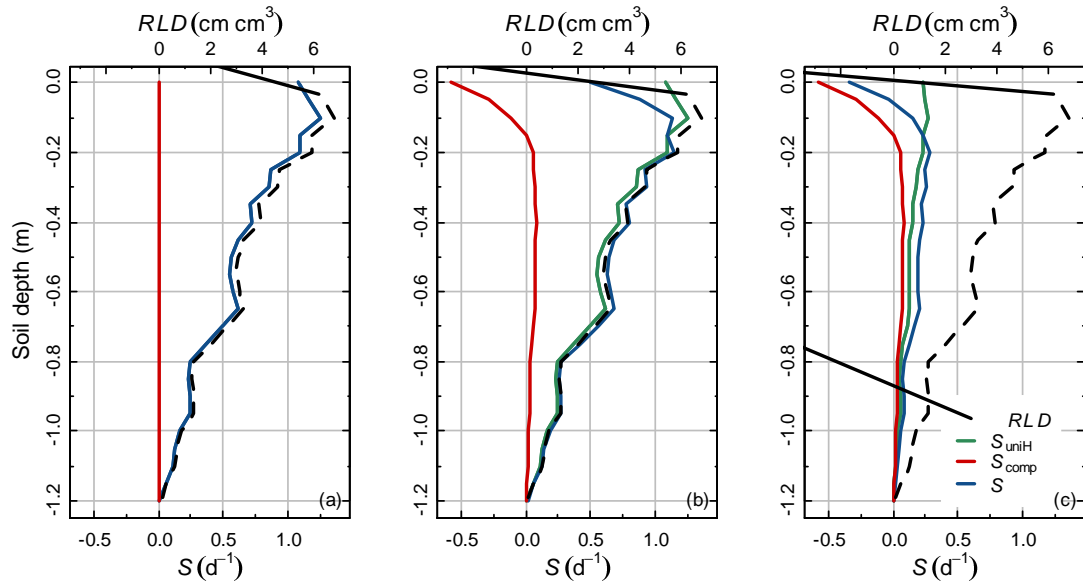
4   **Figure 1: Some examples of root water uptake sink term (S, in d^{-1}) profiles (blue lines) conceptualized as the sum of**
5   **S_{uniH} (green lines), the root water uptake term proportional to root length density *RLD* (dotted black line) and the**
6   **compensatory root water uptake (S_{comp}, red lines). (a) $S_{comp} = 0$ (no root compensation) leading to $S = S_{uniH}$. (b) $S_{comp} \neq$**
7   **0 and becomes negative towards the surface but remains smaller (in absolute term) than S_{uniH}. (c) $S_{comp} \neq 0$ and is**
8   **negative at the surface while is greater than S_{uniH} for z > −0.08 m. In the last case, S is negative at the surface, meaning**
9   **hydraulic lift is observed.**
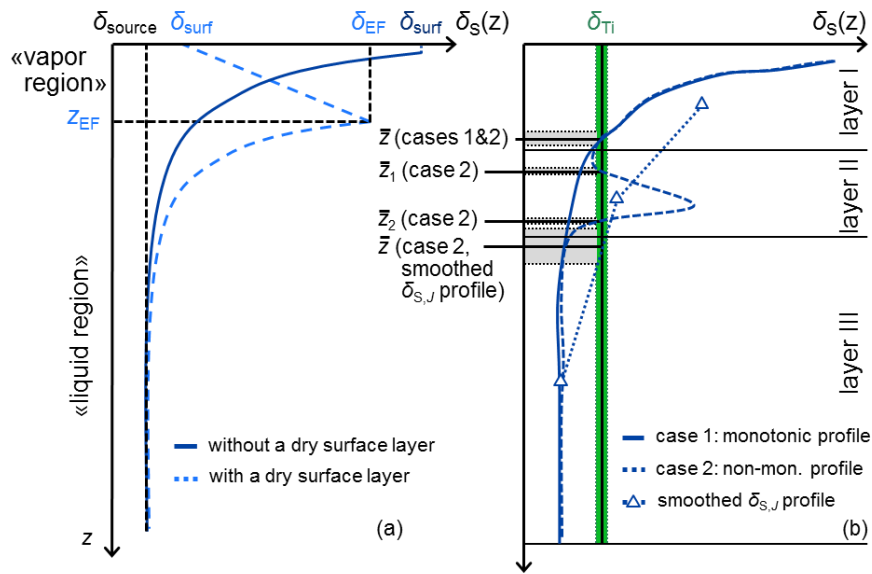
1   **Figure 2**

3   Figure 2: (a) Simulated soil water isotopic composition (δ_S) profiles for a water saturated (dark blue line) and
4   unsaturated (light blue dotted line) soil following Barnes and Allison (1983). Indices "surf" and "EF" refer to soil
5   surface and Evaporation Front. "vapor" and "liquid" regions refer to soil regions where water flow occurs
6   predominantly in the liquid and vapor phase, respectively. (b) Illustration of the "graphical inference" method for
7   determining the "mean root water uptake depth" ($\bar{z}$). "Ti" stands for the sap xylem water at the plant tiller. Case 1:
8   one unique solution is found; case 2: more than one solution is found. Smoothed profile is designated by the symbols).
9    $\bar{z}$ range is indicated by the gray horizontal stripes.

1   **Figure 3**
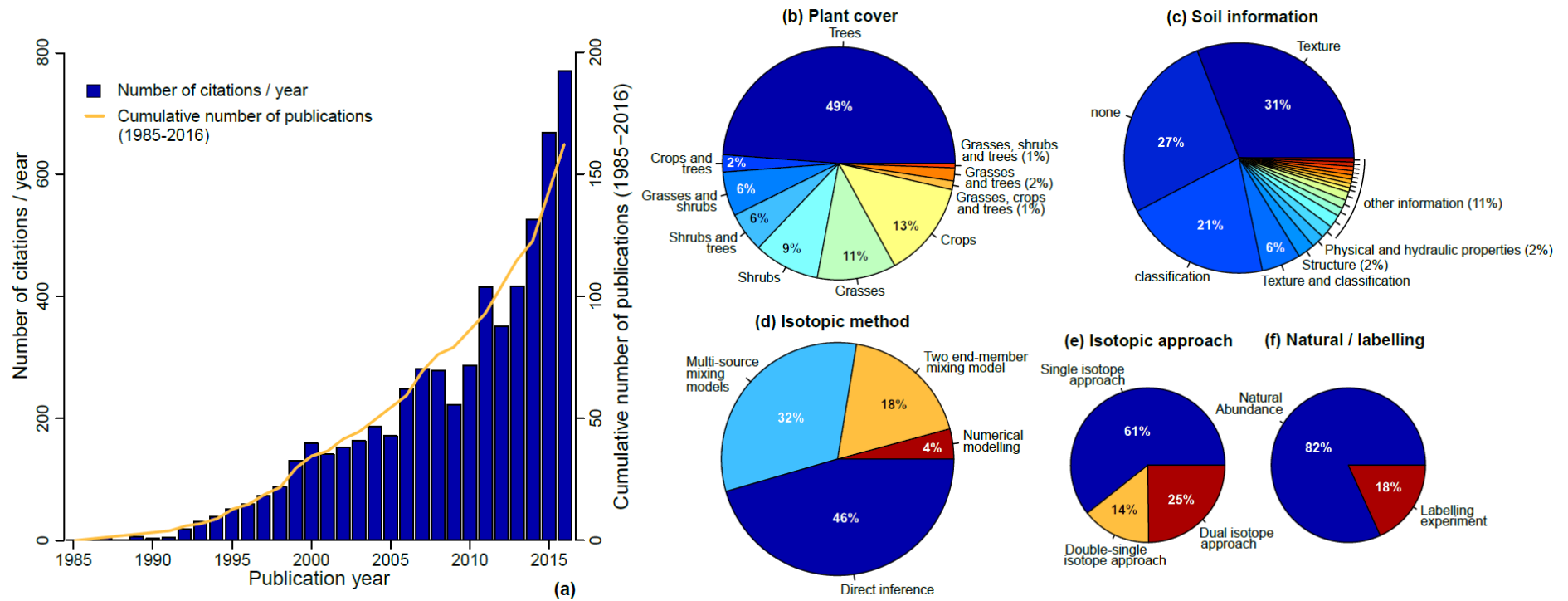
3   **Figure 3: Evolution of the number of citations per year and cumulative number of publications from 1985 to 2016 (a). Details are given on the plant cover (b), the available soil**
4   **information (c), the applied isotopic method (d) and approach (e), and the type of experiment (f).**

1 **Figure 4**
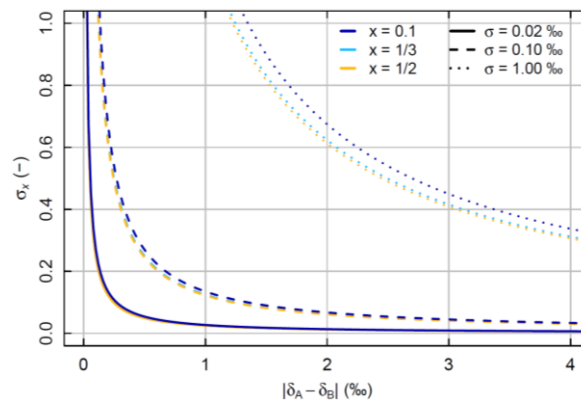
3 **Figure 4: Standard error (σ_x) associated with the estimation of the relative contribution (x) of source A water to root**
4 **water uptake in case of two distinct sources (A and B of isotopic compositions δ_A and δ_B). Three x values (0.1, dark**
5 **blue color; 1/3, light blue; ½, orange) and three values of standard errors associated with sampling and measurement**
6 **of δ_A, δ_B, and of the isotopic composition of the tiller sap water (δ_{Ti}) (0.02, solid line; 0.10 and 1.00, dashed lines) are**
7 **tested.**

1 **Figure 5**
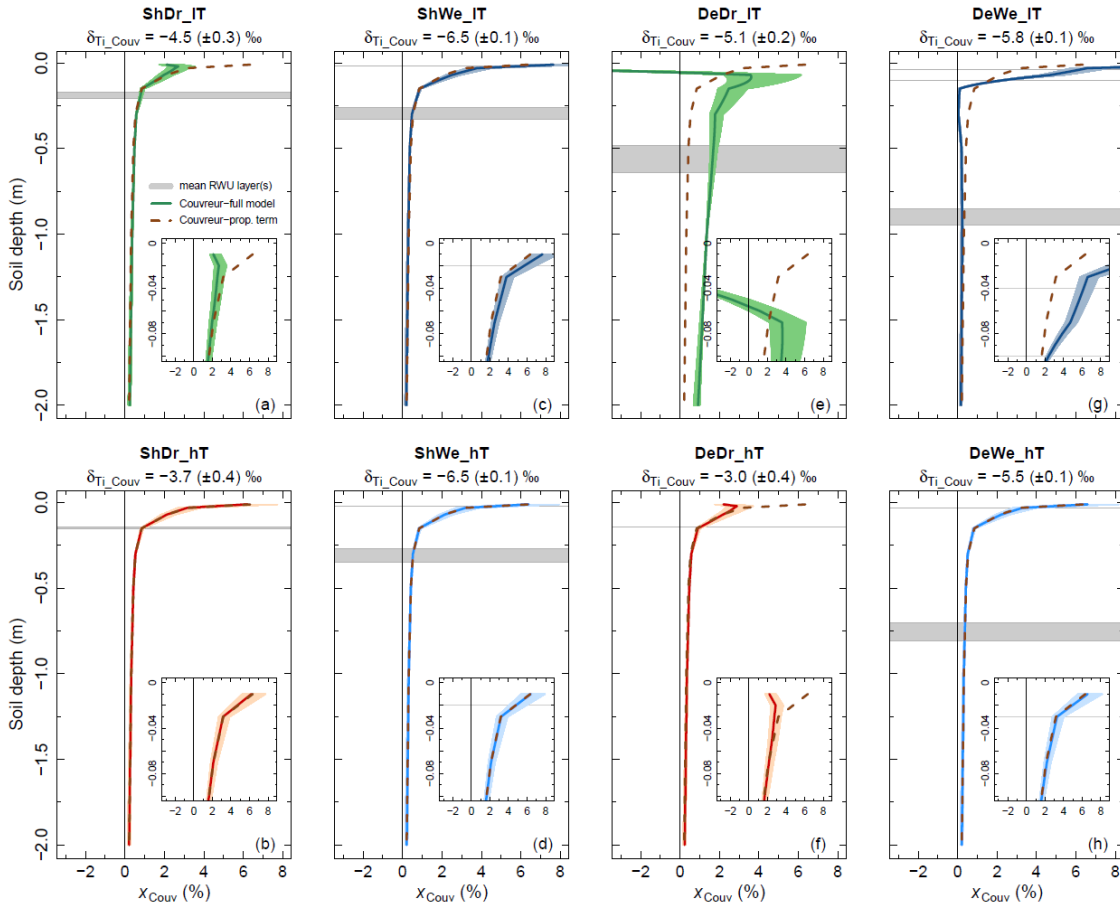
3 **Figure 5: Simulated depth (z, in m) profiles of x_{Couv} (%) (solid colored lines), the simulated relative contributions to**
4 **transpiration provided by the model of Couvreur et al. (2012) for experiments "ShDr" (soil with shallow groundwater**
5 **table and relatively dry soil surface), "ShWe" (soil with shallow groundwater table after a rainfall event)", "DeDr"**
6 **(soil with deep groundwater table with relatively dry soil surface), "DeWe" (soil with deep groundwater table and wet**
7 **soil surface). Suffices "lT" and "hT" refer to "low" and "high" transpiration rate simulations. The color-shaded areas**
8 **depict the uncertainty of the model estimates on the account of the precision of the measurements. The horizontal**
9 **gray-shaded areas delimit the mean root water uptake layer(s) obtained by the "graphical inference" method. At the**
10 **bottom right corner of each plot is a detail presented for $z \geq -0.10$ m. Finally, results from the first term of the model**
11 **of Couvreur et al. (2012) which considers uptake proportional to root length density is plotted as a dashed brown line**
12 **for comparison. Note that negative x_{Couv} means hydraulic redistribution by the roots.**

Figure 6
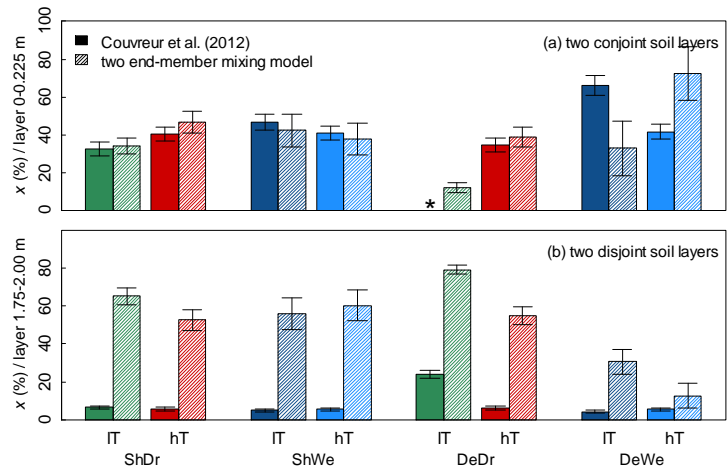
Figure 6: Comparison between relative contributions to transpiration (*x*, in %) simulated by the analytical RWU model of Couvreur et al. (2012) and the two end-member mixing model in case of two defined soil layers. Figure 5a displays *x* from the topmost soil layer (0 – 0.225 m) in case of a two conjoint soil layers (0 – 0.225 m and 0.225 – 2.00 m) whereas Figure 5b displays *x* from the lowest soil layer (1.75 – 2.00 m) in case of a two disjoint soil layers (0 – 0.225 m and 0.225 – 2.00 m), i.e., information on soil water isotopic composition is lacking between 0.225 and 1.75 m. "Sh" ("De") stands for the virtual experiments where the soil has a shallow (deep) groundwater table while "Dr" and "We" stand for when the soil is dry or wet at the surface. Suffices "lT" and "hT" refer to "low" and "high" transpiration rate simulations. "*" refers to when hydraulic redistribution is simulated by the analytical model, leading to a negative *x*. Error bars are either one standard deviation (for the RWU analytical model) or one standard error (for the TM approach).

Figure 7
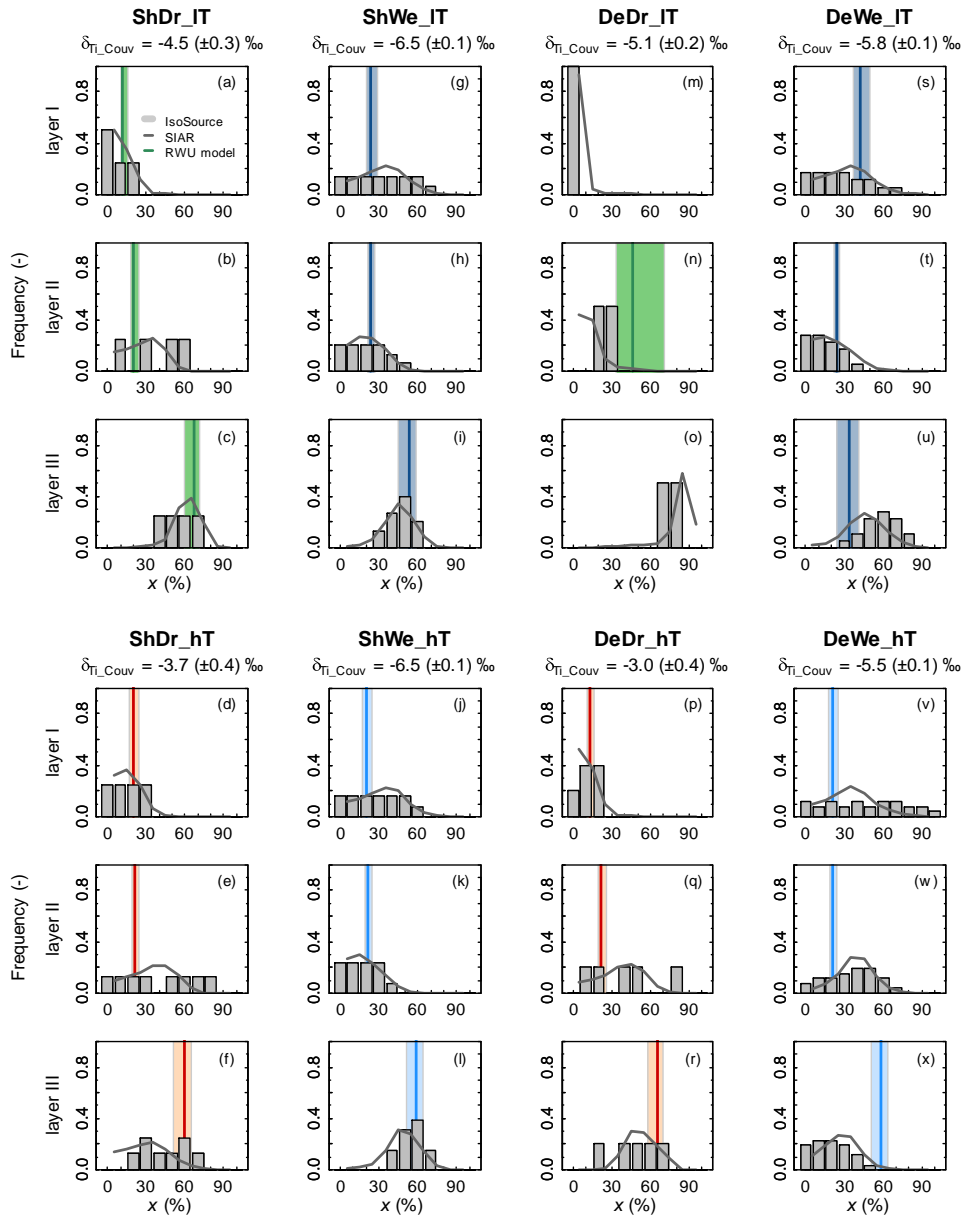
Figure 7: Simulated ranges of possible relative contributions to transpiration from three defined soil layers (I: 0.00 – 0.05 m, II: 0.050 – 0.225 m, and III: 0.225 – 2.000) provided by the multi-source mixing model IsoSource (Phillips and Gregg, 2003) (displayed in the form of gray histograms). Density distribution functions following the Bayesian model SIAR (Parnell et al., 2010) (gray lines). "Sh" ("De") stands for the virtual experiments where the soil has a shallow (deep) groundwater table while "Dr" and "We" stand for when the soil is dry or wet at the surface. Suffices "lT" and "hT" refer to "low" and "high" transpiration rate simulations. The colored vertical lines give x_{I_Couv}, x_{II_Couv}, and x_{III_Couv}, the relative contributions to transpiration from layers I, II, and III simulated by the analytical model of Couvreur et al. (2012). The color-shaded areas associated with x_{I_Couv}, x_{II_Couv}, and x_{III_Couv} refer to their uncertainty associated with input data uncertainty.

APPENDIX

Appendix A: List of symbols

Symbol	Description	Dimension	Equation number	Measured (m) / simulated (s) / prescribed (p)
C, C_S, C_A, C_B, C_{Ti}	Water stable isotopic concentration, soil water stable isotopic concentration, sources A and B water stable isotopic concentrations, xylem sap water isotopic concentration, root water uptake isotopic concentration	$M\,L^{-3}$	2, 3, 6a, 6b	m s
E, E_i	Evaporation rate for $^1H_2^{16}O$ isotopologue, Evaporation rate for $^1H^2H^{16}O$ or $^1H_2^{18}O$ isotopologue	$L^3\,T^{-1}$	B1-B4	m/s
h	Matric head	L		m
H_{eq}, H_L, H_S	Soil water equivalent and leaf water potentials, total soil water potential	P		m
J_A, J_B, J_{Ti}	Fluxes of water originating from water sources A and B, and at the plan tiller	$L^3\,T^{-1}$	6b	m
J_A^i, J_B^i, and J_{Ti}^i	Fluxes of isotopologues originating from water sources A and B, and at the plan tiller	$M\,T^{-1}$	6a	m
K_{plant}, K_{comp}	Plant and compensatory conductances to water flow	$L^3\,P^{-1}\,T^{-1}$	B1-B4	m/p
M_w, M_i	Molar masses of water and isotopologue ($^1H^2H^{16}O$ or $^1H_2^{18}O$)	$M\,L^{-3}$	3	m
RLD RLD_{1D}	Root length density Root length density per unit of surface area	$L\,L^{-3}$ $L\,L^{-1}$	B3	m/p m/p
R_{ref}	Vienna-Standard Mean Ocean Water (V-SMOW) hydrogen or oxygen stable isotopic ratio	-	3	m
S, S_{uniH}, S_{comp},	Total root water uptake sink term as simulated by the analytical model of Couvreur et al. (2012), Root water uptake sink term under uniform soil water potential distribution, compensatory root water uptake sink term.	$L^3\,L^{-3}\,T^{-1}$	1-4, 6b, B4,B5, 6b	s
SSF	Standard sink fraction	-	B2, B4, B4'	m/p
t, Δt	Time, time step	T	11	m
T	Transpiration flux	$L^3\,T^{-1}$	2, 4a, 4b, B1, B3, B4	m
x, x_j x_{Couv}, x_{J_Couv}, x_{J_IsoS}, x_{J_SIAR}	Contributive proportion to transpiration, source j contributive proportion to transpiration, continuous and integrated (layer J) contributive proportions to transpiration as simulated by the analytical model of Couvreur et al. (2012), integrated (layer J) contributive proportions to transpiration as determined by the IsoSource and SIAR models of Phillips and Gregg (2003) and Parnell et al. (2010). Contributive proportion to transpiration under conditions of uniform soil water potential	-	7, 8b, 9, 9'	s
z, z_j, z_{j+1}, Δz_j, z_{max}, $\overline{z}_{RWU}$	Soil depth, soil depth of layers j and $j+1$, thickness of soil layer j, depth of the root system, "mean root water uptake depth"	L	4b, 5, B2-B4'	m/p

Symbol	Description			
δ, δ^2H, $\delta^{18}O$, δ_{source}, δ_{surf}, δ_S, $\delta_{S,j}$, $\delta_{S,J}$, δ_A, δ_B, δ_{Ti}, $\delta_{Ti,m}$, δ_{Ti_Couv}, δ_E	Water stable isotopic composition, water hydrogen and oxygen stable isotopic compositions, source, soil surface, soil water, soil layer *j and J* water isotopic composition, sources A and B water stable isotopic compositions, isotopic composition of xylem sap water at the plant tiller, isotopic composition of xylem sap water measured at the plant tiller, isotopic composition of xylem sap water at the plant tiller as simulated by the model of Couvreur et al. (2012)	- (expressed in ‰)	3-5, 7-9, 11	m/s
ε_j	Residual error term	- (expressed in ‰)	9'	s
θ	Soil volumetric water content	$L^3 L^{-3}$	5, 11	m
ρ	Volumetric mass of water	$M L^{-3}$	3	m
$\sigma_x, \sigma_{\delta_A}, \sigma_{\delta_B}, \sigma_{\delta_{Ti}}$ $\sigma_{\delta_{Ti\_AM}}, \sigma_x$	Sandard errors associated with the measurements of *x*, δ_A, δ_B, δ_{Ti} and estimated uncertainty of δ_{Ti_Couv} as simulated by the analytical model of Couvreur et al. (2012), error associated with the estimation of the contributive proportion to *T* of water source A in the case of two distinct sources	- (expressed in ‰)	8a, 8b	s
τ	Isotopic tolerance	- (expressed in ‰)	10	p

Appendix B: The macroscopic RWU model of Couvreur et al. (2012)

B1: Presentation of the model

In the approach of Couvreur et al. (2012), RWU is based on physical equations describing the water flow processes but without the need of the full knowledge of the root system architecture and local hydraulic parameters. Instead, three macroscopic parameters are needed. The first equation defines plant transpiration:

$$J_{Ti} = K_{plant} \cdot \left(H_{eq} - H_L \right)$$

(B1)

where J_{Ti} [L³ T^{-1}] is the sap flow rate in the root tiller and considered to be equal to the transpiration rate, K_{plant} [L^3 P^{-1} T^{-1}] is the plant conductance to water flow (the first macroscopic parameter of Couvreur et al., 2012's model). H_L[P] is the leaf water potential and H_{eq} [P] the "plant averaged soil water potential" defined as the mean soil water potential "sensed" by the plant root system in the one dimensional (vertical) space:

$$H_{eq} = \int_z SSF(z) \cdot H_S(z)$$

(B2)

where z is the soil depth, H_S [P] is the total soil water potential, and SSF [-] the standard sink term fraction (the second macroscopic parameter of the model of Couvreur et al., 2012). SSF is defined as the RWU fraction under the condition of totally uniform soil water potential (i.e., when $H_S(x,y,z) = H_S$ = cst). Under such conditions, if all the root segments had the same radial conductivity (and the xylem conductance would not be limiting), the RWU distribution in a uniform soil water potential profile would be exactly the same as the root length density per unit of surface area (RLD_{1D} of dimension [L L^{-1}]) profile. SSF could be defined as:

$$SSF(z) = \frac{S_{uniH}(z)dz}{q_{Ti}} \approx \frac{RLD_{1D}(z) \cdot dz}{\int_z RLD_{1D}(z) \cdot dz}$$

(B3)

where $q_{Ti} = J_{Ti}/(\Delta x \Delta y)$ represents the sap flow rate in the root tiller per unit surface area [L T^{-1}], S_{uniH} [T^{-1}] is the RWU sink term under uniform soil water potential profile. The RWU under conditions of heterogeneous soil water potential is described with the following equation:

$$S(z) = S_{uniH}(z) + S_{comp}(z) = q_{Ti} \cdot SSF(z) + K_{comp} \cdot \frac{\left(H_s(z) - H_{eq} \right) \cdot SSF(z)}{V(z)} \qquad \text{(B4)}$$

where K_{comp} [L^3 P^{-1} T^{-1}] is the compensatory conductance and S_{comp} [L^3 T^{-1}] the compensatory RWU accounting for the non-uniform distribution of the soil water potential and $V(z)$ is the volume of soil considered. If the soil water potential is uniform, this term vanishes from the equation, as $H_S = H_{eq}$ for any z, and water is extracted from the soil proportionally to RLD. When the water potential at a certain location is smaller (more negative, which means drier) than H_{eq}, less water is extracted from this location. On the other hand, when the soil is wetter (H_S less negative), a larger amount of water can be taken up from the same location as compared. Note that if $H_S < H_{eq}$ and if the compensatory term is higher than the first one, S can become positive, and water is released to the soil (i.e., hydraulic redistribution). From Eq. (B4), it can be concluded that hydraulic redistribution will preferably occur when q_{Ti} is small and when large soil water potential gradients exist. Plant root hydraulic characteristics will control compensation through the K_{comp} term. The importance of the compensatory RWU

term has been discussed in the literature for a long time (e.g., Jarvis, 1989). Except if plants activate specific mechanisms to avoid it, compensation always takes place under natural conditions due to the spatially heterogeneous distribution of soil water potential (Javaux et al., 2013).

A simplifying hypothesis that can be made (Couvreur et al., 2014; Couvreur et al., 2012) is to consider that K_{plant} and K_{comp} are equal, which substituted in Eq. (B4) leads to:

$$S(z) = SSF(z) \cdot K_{plant} \cdot \left(H_s(z) - H_L \right) / V(z)$$

(B4')

Finally, the uptake of water stable isotopologues, i.e., the "isotopic sink term" (S_i [M T^{-1}]) is defined as:

$$S_i(z) = S(z) \cdot C(z)$$

(B5)

where C [M L^{-3}] is the water isotopic concentration.

B2: Running the model for the inter-comparison

The root water uptake (S) depth profiles and corresponding δ_{Ti_Couv} were simulated using the model of Couvreur et al. (2012) (Eq. (B4')) for all eight scenarios. For this, H_S, δ_S, and RLD input data were interpolated at a 0.01 m vertical resolution and the resistance of the xylem vessels was assumed to be neglible so that $H_{Ti} = H_L$. A K_{plant} value of 2.47 10^{-6} h^{-1} was taken and was determined based on concomitant T, H_{eq} and H_L data measured for *Festuca arundinacea*. δ_{Ti_Couv} was then calculated from Eq. (4b) (section §2.3). From these simulations, the depth profiles of x_{Couv} (%), the ratio $\dfrac{S(z)dz}{T/(\Delta x \cdot \Delta y)}$ at each interpolated depth z was determined, and x_{J_Couv}, the ratio

$\dfrac{S(z)dz}{T/(\Delta x \cdot \Delta y)}$ from each of the integrated soil layers J ($J \leq$ III or $J \leq$ VIII) were calculated. In order to account for uncertainty of the input data (i.e., total soil water potential and oxygen isotopic composition H_S and δ_S, and root length density RLD), the model was run a 1000 times where a single offset randomly selected between −5 and +5 cm, −0.2 and +0.2 ‰, and −0.1 and +0.1 cm cm^{-3} was added to the initial values (reported Table 2) of H_S, δ_S, and RLD, respectively. By doing this we obtained *a posteriori* distributions of S and corresponding δ_{Ti_Couv} standard deviations ($\sigma_{\delta_{Ti\_Couv}}$);

Appendix C: Inter-comparison methodology

The graphical inference method (GI), the two end-member mixing model (TM), and the multi-source mixing models IsoSource (Phillips and Gregg, 2003) and SIAR (Parnell et al., 2010) were compared to each-other in the following manner for each of the eight virtual experiments:

5   (i)   Single (or multiple) mean RWU depth(s) ($\bar{z}$) were graphically identified following the GI method as the depth(s) of the intersection between a vertical line of value δ_{Ti_Couv} with the δ_S profile. The uncertainty of method GI was determined on the basis of the δ_{Ti_Couv} *a posteriori* distribution: by taking into account $\sigma_{\delta_{Ti\_Couv}}$, $\bar{z}$ results were translated into "RWU layers";

(ii)   relative contribution of RWU to transpiration (x_{TM}, %) to two defined soil layers (either conjoint: $0 - 0.225$

10   m and $0.225 - 2.00$ m or disjoint: $0 - 0.225$ m and $1.75 - 2.00$ m) were determined using the TM approach. For this, representative values for the water oxygen isotopic compositions of these soil layers were computed using Eq. (5) which uses soil volumetric water content (θ, in $m^3\,m^{-3}$) as input data. θ distribution was obtained from H_S distribution and the van Genuchten (1980) closed-form equation. Values for its different parameters, i.e., the soil residual and saturated water contents (θ_{res} and θ_{sat}), and the shape

15   parameters related to air entry potential and pore-size distribution (α and n) were equal to 0.040 and 0.372 $m^3\,m^{-3}$, 0.003 cm^{-1}, and 3.3, respectively;

(iii)   Possible range of x_{J_IsoS}, the relative contribution of RWU to transpiration for each of the integrated soil layers following the IsoSource model was computed based on smoothed $\delta_{S,J}$ profile and δ_{Ti_Couv} by solving the following equation:

$$\sum_J x_{J\_IsoS} \cdot \delta_{S,J} \leq \left| \delta_{Ti\_Couv} \pm t \right|$$

     (C1)

with $\tau = \sigma_{\delta_{Ti\_Couv}}$.

$\delta_{S,J}$ was computed similarly to for the TM method;

(iv)   Density distribution of x_{J_SIAR}, the relative contribution of RWU to transpiration for each of the three (or

25   eight) soil layers following the SIAR model was determined based on smoothed $\delta_{S,J}$ profile and δ_{Ti_Couv} data as well. To compare with the IsoSource model (i) the number of δ_{Ti} replicates was fixed to three and equal to $\delta_{Ti\_Couv} - \sigma_{\delta_{Ti\_Couv}}$, δ_{Ti_Couv}, and $\delta_{Ti\_Couv} + \sigma_{\delta_{RWU\_Couv}}$, and (ii) x_{J_SIAR} was computed at a 10% increment (i). No prior information on the relative contributions to T was used to run the model, i.e., we opted for flat priors;

30   (v)   Results obtained at steps (i)-(iv) were compared to each other;

(vi)   Sensitivity of IsoSource to the values of i and τ, and of SIAR to values of arguments *iterations* and *burnin* were finally briefly tested.